






The choice of targets and ligands for site-specific delivery of nanomedicine to atherosclerosis

Adil Zia ¹, Yuao Wu ^{1,2}, Tuan Nguyen³, Xiaowei Wang ⁴, Karlheinz Peter ⁴, and Hang T. Ta ^{1,2*}

¹Australian Institute for Bioengineering and Nanotechnology, The University of Queensland, Brisbane, QLD 4072, Australia; ²School of Pharmacy, Pharmacy Australia Centre of Excellence, The University of Queensland, Woolloongabba, QLD 4102, Australia; ³School of Chemical Engineering, The University of Queensland, Brisbane, QLD 4072, Australia; and ⁴Baker Heart and Diabetes Institute, Melbourne, VIC 3000, Australia

Received 30 October 2019; revised 23 December 2019; editorial decision 25 January 2020; accepted 17 February 2020; online publish-ahead-of-print 20 February 2020

Abstract

As nanotechnologies advance into clinical medicine, novel methods for applying nanomedicine to cardiovascular diseases are emerging. Extensive research has been undertaken to unlock the complex pathogenesis of atherosclerosis. However, this complexity presents challenges to develop effective imaging and therapeutic modalities for early diagnosis and acute intervention. The choice of ligand-receptor system vastly influences the effectiveness of nanomedicine. This review collates current ligand-receptor systems used in targeting functionalized nanoparticles for diagnosis and treatment of atherosclerosis. Our focus is on the binding affinity and selectivity of ligand-receptor systems, as well as the relative abundance of targets throughout the development and progression of atherosclerosis. Antibody-based targeting systems are currently the most commonly researched due to their high binding affinities when compared with other ligands, such as antibody fragments, peptides, and other small molecules. However, antibodies tend to be immunogenic due to their size. Engineering antibody fragments can address this issue but will compromise their binding affinity. Peptides are promising ligands due to their synthetic flexibility and low production costs. Alongside the aforementioned binding affinity of ligands, the choice of target and its abundance throughout distinct stages of atherosclerosis and thrombosis is relevant to the intended purpose of the nanomedicine. Further studies to investigate the components of atherosclerotic plaques are required as their cellular and molecular profile shifts over time.

Keywords

Atherosclerosis • Targets • Ligands • Binding affinity • Nanoparticles

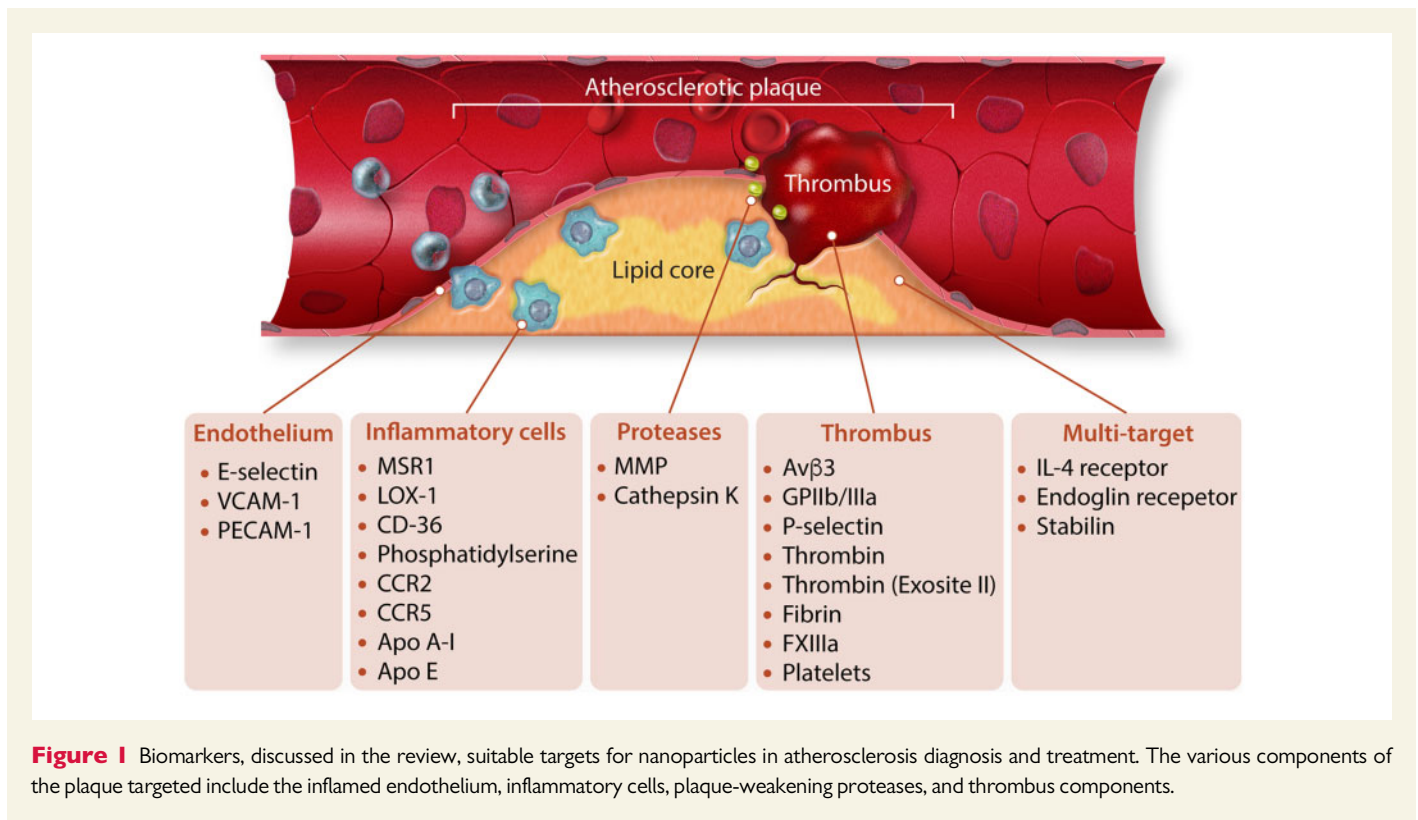
1. Introduction

Cardiovascular diseases (CVDs) are a major cause of death worldwide. With an estimated 17.7 million deaths in 2015, CVDs contributed to 31% of global deaths; of which 7.4 million were due to coronary heart disease, and 6.7 million were due to stroke.¹ CVDs are often associated with developed countries; however, the incidence in the developing world is also increasing. The primary cause of cardiovascular dysfunction is atherosclerosis—a progressive disease involving the deleterious accumulation of lipids and fibrous elements within the arterial wall (Figure 1). An imbalance in cholesterol metabolism and a maladaptive immune response initiate and progress the formation of an atherosclerotic plaque. Risk factors include smoking, hypertension, high cholesterol, obesity, diabetes mellitus, and so on.² Once established, an atherosclerotic plaque can develop into either a stable plaque or an unstable (vulnerable) plaque.³ Vulnerable plaques generally have thin fibrous caps and are prone

to rupture and can subsequently cause thrombosis, obstructing the lumen and leading to acute ischaemic events.⁴

Recent advances in nanotechnology and nanomaterial science have provided novel tools for advanced therapy and diagnosis of vascular diseases.⁵ Nanomaterials are often inorganic and organic particles with spherical, cylindrical, plate-like, or other morphologies that are usually between 1 and 100 nm in diameter. Nanomaterials have been typically developed to function as drug carriers or imaging contrast agents. Nanomaterials with size in the range of 50–150 nm can be easily accumulated at disease sites due to the enhanced permeability and retention (EPR) effect.⁶ Moreover, they can be labelled with binding ligands that specifically target disease biomarkers for targeted delivery of therapeutics and for diagnostic molecular imaging of diseases, thus enhancing the specificity of the therapy and the detection. The use of binding ligands, such as small molecules, peptides, aptamers, and antibodies, modulate the biodistribution of these nanoparticles.⁷ Due to relatively large

* Corresponding author. Tel: +61 7 3346 1720, E-mail: h.ta@uq.edu.au, hangthuta@gmail.com



surface area-to-volume ratio, nanoparticles can carry high density of not only single type of ligand but also an incorporation of multiple ligands.

Atherosclerosis can remain asymptomatic for many years, whose symptoms only arise when the occlusion interferes with the circulation and blood supply to tissues. However, this mechanism accounts for only 30–40% of acute events. The majority (60–70%) of patients suffer from thrombosis-related acute coronary syndrome or sudden ischaemic death. Therefore, being able to effectively assess the vulnerability of rupture-prone plaques could greatly improve clinical outcomes. Vascular targeting has been used for localized delivery of therapeutics primarily in cancer treatments, but also increasingly in both diagnosis and therapy of CVDs. The earliest binding ligand used in CVDs was arginyl-glycyl-aspartic acid (RGD), which can be recognized by integrins. Its discovery can date back to the last century.⁸ This small sequence of peptide was soon used in thrombus imaging.⁹ Since then, numerous binding ligands have been developed for targeting purpose in the diagnosis and treatment of CVDs. Accordingly, a wide range of cell types, cellular and molecular processes involved in atherosclerosis can serve as local targeting epitopes (Figure 1). A right choice of highly specific ligand-receptor targeting system is, therefore, crucial in developing functionalized nanoparticles for the diagnostic and therapeutic purposes.

This review will discuss the plethora of target receptors presenting throughout the atherosclerosis and the effectiveness of current binding ligands developed to target nanomaterials to various components of an atherosclerotic plaque is summarized in Table 1. The effectiveness of the ligands will be assessed by their binding affinity and selectivity to targets expressed at the disease site: K_d —the dissociated constant describing the affinity between a ligand and target, K_i —the inhibition constant indicating the concentration required to produce half-maximum inhibition, IC_{50} —the concentration of inhibitor required to reduce binding by half, and K_{cat}/K_m ratio—the catalytic efficiency.

2. Passive targeting

In addition to active targeting approaches, passive targeting based on the EPR effect is also an important targeting method for nanomaterials. In atherosclerosis, angiogenesis plays an important role in the development of the disease. When abnormal angiogenesis occurs, it will be accompanied by the rapid proliferation of endothelial cells, so atypical blood vessels with structural defects are formed. This increases vascular permeability within atherosclerotic plaques and allows nanoparticle to pass into the interstitial tissue easily. At the same time, the lymphatic system can help the accumulation of nanoparticles, which eventually increases the local drug concentration in the diseased area.⁶⁶ Since atherosclerosis is an inflammatory disease, atherosclerotic plaques attract white blood cells by releasing pro-inflammatory cytokines. As leucocytes continue to traverse the endothelium into the intima of the blood vessel, the permeability of the endothelium is increased, which allows selective delivery of the nanocarriers to the site of inflammation. Recent studies show that some nanocarriers can effectively reach the site of myocardial ischaemia–reperfusion through enhanced vascular permeability with the cooperation of monocytes and macrophages.^{67,68}

3. Targeting inflamed endothelial cells

Upon inflammatory stimulation, the permeability of the endothelium increases, allowing molecules to extravasate and localize into the interstitial space. In addition, endothelial cells begin to express various types of adhesion molecules, such as selectins and integrins, which recruit leucocytes to the site of inflammation.⁶⁹

Table 1 Summary of interactions between targets and ligands reviewed

Targets	Ligands	Format	K _d	K _i	IC ₅₀	K _{cat} /K _m
Endothelial cells						
E-selectin	ESTA-1 ¹⁰	DNA Thioaptamer	47 nM	–	–	–
VCAM-1	antiVLA-4: VHSPNKK ^{11,12}	Peptide	39.6 nM	–	–	–
	antiVLA-4: CNNSKSHTC ^{12,13}	Cyclic peptide	37.2 nM	–	6.14 nM	–
	antiVLA-4: VHPKQHR ¹⁴	Oligopeptides	–	–	–	–
	scFv _{in} VCAM-1 ¹⁵	Single-chain fragment variable (ScFv)	–	–	–	–
PECAM-1	Heparin ¹⁶	Oligosaccharide	4.93 nM	–	–	–
	Anti-PECAM antibody ¹⁷	Antibody	–	–	–	–
ICAM-1	Anti-ICAM-1 VHH single-domain antibody (sdAb) ¹⁸	Antibody	–	–	–	–
	ICAM-1 Monoclonal Antibody ¹⁹	Antibody	–	–	–	–
	Anti-ICAM-1 antibody ^{20,21}	Antibody	–	–	–	–
	γ3: NNQKIVNLKVKVAQLEA ²²	Peptide	–	–	–	–
CD81	Anti-CD81 antibody ²³	Antibody	–	–	–	–
Inflammatory cells						
MSR1 (CD204)	Anti-MSR1 (anti-CD204) monoclonal antibody ²⁴	Antibody	–	–	–	–
LOX-1	Anti-LOX-1 antibody ²⁵	Antibody	–	–	–	–
CD36	EP80317: Haic-D-2MeTrp-D-Lys-Trp-D-Phe-Lys-NH2 ^{26,27}	Peptide	–	–	14 nM	–
	Anti-CD36 antibody ²⁶	Antibody	–	–	–	–
Apo A-I mimetic	37pA: DWLKAFYDKVAEKLEAFPDWLKAFYDKVAEKLEAF ²⁸	Peptide	–	–	–	–
	18A: DWLKAFYDKVAEKLEAF ²⁸	Peptide	–	–	–	–
Apo E	P2fA2: LRKLRKLLR ²⁹	Peptide	–	–	–	–
CRR2	YNFTNRKISVQRLASVRRITSSK ³⁰	Peptide	–	–	–	–
CRR5	ASTTTNYT ³¹	Peptide	–	–	–	–
Folic acid receptor β on macrophage	Folic acid ^{32,33}	Small molecule	–	–	–	–
PS	Annexin V ^{34–36}	Protein	pM–fM	–	–	–
Proteases						
MMP	CGS 25966 ³⁷	Hydroxamate	–	11–43 nM	–	–
	CGS 27023A ³⁷	Hydroxamate	–	8–43 nM	–	–
	P947: Gly-Pro-D-Leu-D-Ala-NHOH ³⁸	Peptide	–	–	μM range	–
	Gelatinase substrate (GGPRQITAG) ³⁹	Peptide	–	–	–	0.18 × 10 ⁶ M ⁻¹ s ⁻¹
Cathepsin K	CatK substrate (GHPGGPQKGC) ⁴⁰	Peptide	1.2 μM	–	–	–
Thrombus						
α _v β ₃	Vitronectin ⁴¹	Protein	–	μM range	–	–
GPIIb/IIIa	RGD ⁴²	Peptide	–	–	>100 nM	–
	P280: containing RGD mimetic sequence (D-Tyr)-Apc-Gly-Asp-NH (Apc is S-aminopropyl-L-cysteine, a synthetic amino acid) ⁹	Peptide (cyclic)	–	–	79 nM	–

Continued

Table 1 Continued

Targets	Ligands	Format	K _d	K _i	IC ₅₀	K _{cat} /K _m
P-selectin	P748: sequence containing (D-Tyr)-Amp-Gly-Asp-NH (Amp is 4-amidinophenylalanyl, a synthetic amino acid) ⁴³	Peptide (cyclic)	—	—	28–36 nM	—
	P977: CRGDC ⁴⁴	Peptide (cyclic)	—	1.1 μM	—	—
	DMP728 N-methyl-L-arginyl-glycyl-L-aspartyl ⁴⁵	Peptide (cyclic)	0.1 nM	0.4 nM	4.6 nM	—
	DMP757 cyclo(D-Val-NMe-Arg-Gly-Asp-Mamb) ⁴⁶	Peptide (cyclic)	—	—	6 nM	—
	Anti-GPIIb/IIIa scFv ^{47–50}	scFv	—	—	—	—
	Fucoidan ⁵¹	Sulfated polysaccharide	0.3–1.2 nM	—	—	39.4 × 10 ⁶ M ⁻¹ s ⁻¹
	Cleavable ligand: GPXRSGGGK ⁵²	Peptide	—	—	—	—
	Cleavable ligand: KKLVRGSL ⁵³	Peptide	—	—	—	—
	ODN2 ⁵⁴	DNA aptamer	0.5 nM	—	—	—
	SbO4L: Ac-GDFEIEE-γ(SO3H)-LQ ⁵⁵	Peptide	—	—	14 nM	—
Fibrin	H6 ⁵⁶	scFv	199 nM	—	—	—
	Di-80B3 ^{57,58}	Monoclonal antibody antigen-binding fragment (Fab)	1.6 nM	—	—	—
	1H10 ⁵⁹	Antibody	8.04 nM	—	—	—
	5F3 ⁵⁹	Antibody	11.3 nM	—	—	—
	AP2 ⁶⁰	Antibody	44 nM	—	—	—
	TP850: GPRPP ⁵¹	Pentapeptide	8 nM	—	—	—
	EP-2104R: YQCPYGLCYIQ ⁶¹	Peptide	1.6 μM	—	—	—
	Anti-fibrin Fab' fragment (against D-dimer region) ⁵⁷	Antibody	1.6 nM	—	—	—
	A15: N ₁₃ QEQVSP ₁ LLK ₂₄ ⁶²	Peptide	—	—	—	—
	Multi-target	BMP-9 ⁶³	Protein	2–10 nM	—	—
IL-4 (CRKRLDRNC) ⁶⁴		Peptide	100–150 pM	—	—	—
CRTLTVRK ⁶⁵		Peptide	—	—	—	—

IC₅₀, functional strength of an inhibitor; K_{cat}/K_m, catalytic efficiency of enzyme-substrate reaction; K_d, binding affinity of a ligand; K_i, binding affinity of an inhibitor.

Vascular cell adhesion protein 1 (VCAM-1) is a cell adhesion molecule that is overexpressed on the surface of inflamed endothelial cells. It mediates the recruitment of monocytes to the plaque and involved in the inflammatory process. Hence, VCAM-1 expression can be correlated with the extent of exposure to atherosclerotic risk factors. Serum concentrations of soluble VCAM-1 in patients with atherosclerotic diseases can reach >800 ng/mL.⁷⁰ VCAM-1 exhibits a high affinity ($K_d = 39.6$ nM) for very-late antigen-4 (VLA-4). Upon expressed on the surface of leucocytes, VLA-4 interacts with VCAM-1 causing leucocyte adhesion to vascular endothelium. Kelly *et al.*^{71,72} synthesized magnetofluorescent nanoparticles functionalized with a peptide whose sequence VHSPNKK homologous to the α -chain of VLA-4. This peptide-conjugated nanoparticle was the first endothelial imaging agent that was not functionalized with anti-VCAM-1 mAbs. Moreover, the target-to-background ratio achieved by this probe was 12-fold higher compared to mAb-based probes. Nahrendorf *et al.*¹¹ adapted the VHSPNKK motif to produce another peptide (VHPKQHR) that exhibited higher cellular internalization, enhancing magnetic resonance imaging (MRI) resolution and optical imaging. Employing this peptide, Bruckman *et al.*¹⁴ showed that VCAM-1 targeted tobacco mosaic virus (TMV) carrying both near-infrared dye and chelated gadolinium (Gd) ions were highly accumulated in atherosclerotic plaques of ApoE^{-/-} mouse. The VHPKQHR peptide-conjugated TMV nanoparticles with loaded of gadolinium contrast agent required 400 times lower dose to achieve the desired results of MRI compared to the suggested clinical use of Gd.

Another endothelial-targeting MRI contrast agent was synthesized in the form of ultra-small superparamagnetic iron oxide (USPIO) NPs functionalized with VCAM-1-targeting heptapeptide NNSKSHT. This VCAM-1-targeting USPIO NP was reported to reach vulnerable plaques within 30 min post-injection. ELISA and blocking experiments determined a K_d of 37.2 nM and an IC_{50} of 6.14 nM, respectively.¹² The same cyclical heptapeptide (NNSKSHT) was studied by Michalska *et al.*¹³ for the detection of early and advanced atherosclerotic lesions in ApoE^{-/-} mice. Accordingly, the USPIO NPs displayed enhanced contrast, increased spatial resolution, and precise localization in atherosclerotic lesions and VCAM-1 expression endothelial cells.

In addition to peptides, single-chain antibodies can also be used to localize VCAM-1 in endothelial cells. Wang *et al.*¹⁵ conjugated VCAM-1 single-chain fragment variable antibodies (ScFv) to the microbubbles (MBs) with loading of miR-126 mimetic as a therapeutic drug. *In vivo* studies indicated that anti-VCAM-1 scFv labelled MBs had stronger contrast intensity of ultrasound imaging in angiotensin (Ang)-II-induced AAA murine model than the PBS control mice. Simultaneously, anti-VCAM-1 ScFv labelled MBs could also enrich miR-126 in activated endothelial cells.

E-selectin is another cellular adhesion molecule expressed only on endothelial cells activated by inflammatory molecules, such as tumour necrosis factor- α (TNF- α), interleukin-1, and LPS. E-selectin is known as CD62 antigen-like family member E (CD62E), endothelial-leucocyte adhesion molecule 1 (ELAM-1), or leucocyte-endothelial cell adhesion molecule 2. The lectin-like domain and epidermal growth factor-like domain of E-selectin are thought to mediate binding of leucocytes as they 'roll' along the endothelium.⁷³ The maximal expression of E-selectin occurs 4 h after stimulation and rapidly decreases thereafter. Evidence suggests that E-selectin expression occurs in 35% of fibrous plaques and 22% of lipid-containing plaques.⁷⁴ Some of the ligands recognized by E-selectin include E-selectin ligand-1 (ESL-1), P-selectin glycoprotein-1 (PSGL-1), L-selectin, cluster of differentiation 43/leucosialin (CD43) cluster of differentiation 44 (CD44), β 2-integrins, and death receptor-3

(DR3). PSGL-1 initiates leucocyte capture, whereas ESL-1 converts initial tethers into slow steady rolling, with CD44 controlling the velocity.⁷⁵ Sialyl lewis^x (SLE^x) and Sialyl lewis^a (SLE^a) are carbohydrate motifs that are also recognized by E-selectin. Mann *et al.*¹⁰ reported an E-selectin thioaptamer ligand (ESTA-1) that also selectively recognizes E-selectin. The thioaptamer had nanomolar affinity ($K_d = 47$ nM) in conjunction with minimal cross-reactivity with P- and L-selectin.

Platelet endothelial cell adhesion molecule 1 (PECAM-1) and intercellular adhesion molecule 1 (ICAM-1) are also mediators of leucocyte migration from the blood vessel into the endothelium and intima. Studies have shown that there are two binding regions in PECAM-1 that appear to have a very high affinity for heparin oligosaccharides ($K_d = 4.93$ nM).¹⁶ Dziubla *et al.*¹⁷ conjugated anti-PECAM antibody on the surface of polymer nanocarriers loaded with catalase. Targeting experiments showed that the anti-PECAM-polymer nanocarriers bound endothelial cells nearly 10 times more efficiently than non-targeted polymer nanocarriers.

Bertrand *et al.*¹⁸ conjugated anti-ICAM-1 single-domain antibodies (sdAb) to their molecular probes for near-infrared fluorescence (NIRF) imaging and showed that the ICAM-1 targeted probe exhibited NIRF signals at 1.47-fold and 4.7-fold higher than the non-targeted probe *in vivo* and *ex vivo*, respectively. Herbst *et al.*¹⁹ developed bifunctional echogenic immunoliposomes (BF-ELIP) by covalently coupling both ICAM-1, monoclonal antibody (mAb), and rabbit CD34 polyclonal antibody to the lipid system. The purpose of this design is to allow the lipid system to bind to the endothelial cells at one end and to the stem cells at the other end, thus targeting stem cells to endothelial cells, helping the regeneration and repair of damaged tissues. The experimental results show that ICAM-1 mAb could effectively help the delivery of stem cells-bound liposomes to the arterial wall. Some similar studies have shown that ICAM-1 antibody-conjugated liposomes could effectively deliver computed tomography (CT)²⁰ and MRI²¹ contrast agents to the vascular endothelium. In addition to antibodies, peptide has also been developed to target ICAM-1. A study by Garnacho *et al.*²² found that a linear peptide derived from fibrinogen (γ 3) NNQKIVNLKEKVAQLEA has a similar targeting effect as anti-ICAM-1 antibody.

Recent evidence indicates that CD81, a ubiquitous tetraspanin protein, is up-regulated in the endothelium of atherosclerotic human arteries.⁷⁶ Micron-sized iron oxide particles (MPIO) have been functionalized with anti-CD81 antibody, which confers high specificity and binding affinity to the target. Each MPIO was conjugated with 1.5×10^5 antibody molecules, resulting in approximately 18.26 MPIO bound to PMS-stimulated murine endothelial cells. A 10-fold and 100-fold increase in conjugated antibody molecules per MPIO resulted in approximately 180 and 940 particles bound to cells, respectively.²³

Thapa *et al.*⁷⁷ found that peptide CLWTVGGGC was able to specifically target bovine aortic endothelial cells (BAECs) treated with TNF- α or LPS but not to the cells activated by other inflammatory cytokines including IL-1 or IL-4. BAECs with those cytokines did not induce VCAM-1 expression in the cells. However, the binding of this peptide to other endothelial cells such as HUVECs (human umbilical venous endothelial cells) and HLECs (human lymphatic endothelial cells) were significantly low although the cells were also treated with TNF- α , and VCAM-1 was expressed on these cells. It suggested that CLWTVGGGC is specific to aortic endothelial cells activated by TNF-alpha and LPS, but it is still unclear which epitope(s) on the cells the peptide bind to. *In vivo*, compared to normal mice, the CLWTVGGGC peptide showed approximately five-fold higher homing to aortic tissue of Ldlr^{-/-} mice, co-localized with endothelial cells overlying atherosclerotic plaque, after 1-h

circulation. The distribution of the peptide, however, was observed inside a plaque as well as along the aortic endothelial cells overlying the plaque. Interestingly, the homing of CLWTVGGGC peptide to control organs such as lung and liver was minimal, while considerably present in kidney probably because kidney is the major excretory route for peptides.

4. Targeting inflammatory cells

Inflammatory cells are involved throughout atherosclerosis, thrombosis, and plaque destabilization. The microenvironment of the macrophage can influence its phenotype: M1 may result in plaque vulnerability, M2 may increase plaque stability.⁷⁸ Immunohistological studies indicate higher macrophage density in atherosclerotic plaques obtained from patients with the recent acute coronary syndrome than patients with stable CVD.⁷⁹

Monocytes in atherosclerosis are an ideal target cell because the influx of monocytes is a marker of early lesions. Furthermore, accumulation of monocytes is associated with progression of the disease, and plaques that are prone to rupture have a higher number of monocytes.⁸⁰ The chemokine receptor on the surface of monocytes will aggregate during the course of the disease, so it is a good biomarker.⁸¹ Chung et al.³⁰ constructed peptide amphiphile micelles (PAMs) labelled with YNFTNRKISVQRLASYRRITSSK that can target monocyte C-C chemokine receptor 2 (CCR2). The results indicated that, after 24 h of cycling, the targeted PAMs could effectively accumulate at the atherosclerotic plaques in the ApoE^{-/-} mouse. Similarly, Luehmann et al.³¹ conjugated the monocyte C-C chemokine receptor 5 (CCR5) binding peptide ASTTTNYT [D-Ala1-peptide T-amide (DAPTA)] to the comblike nanoparticles and compared the biodistribution and quantitative uptake of comblike nanoparticles with or without DAPTA binding (Cu-DOTA-comb/Cu-DOTA-DAPTA-comb). Positron emission tomography (PET) and CT results demonstrated that the particles labelled with the CCR5 targeting peptide had a higher targeting efficiency at the vascular injury sites in mouse than the one without the targeting peptide ligand.

Macrophages bind and uptake low-density lipoprotein (LDL) and oxidized LDL (oxLDL) via scavenger receptors, such as macrophage scavenger receptor 1 (MSR1), CD36 receptor, and lectin-like oxidized receptor (LOX-1). Overexpression of these receptors positively correlates with plaque instability and vulnerability.⁸² Amirbekian et al.²⁴ chose MSR1 (CD204) as a target for molecular MRI of atherosclerotic lesions. Accordingly, Gd-immunomicelles were functionalized with anti-MSR1 (anti-CD204) monoclonal rat anti-mouse antibody. *In vivo* MRI found that at 24 h post-injection, the macrophage-targeted immunomicelles increased the signal intensity of the atherosclerotic vessel wall in ApoE^{-/-} mice by 79% compared with untargeted micelles (34%). EP80317 (Haic-WKWFK), derived from the growth hormone-releasing peptide family, has a high affinity ligand (IC₅₀ = 14 nM) for CD36 receptor. Administration of this peptide ligand was able to attenuate the progression of atherosclerosis in ApoE^{-/-} mice (>50% reduction in lesion size) through the blockage of oxLDL binding site.⁸³ CD36 targeting was also achieved by using anti-CD36 antibody incorporated on the surface of Gd lipid-based nanoparticles. *In vitro* studies found that this functionalized nanoparticle had high uptake in human macrophages and increased signal intensity in human atherosclerotic lesions in *ex vivo* studies.²⁶ Wen et al.²⁵ used USPIO functionalized with anti-LOX-1 antibody for non-invasive MRI of carotid atherosclerotic lesions. The study showed that the lesions could be imaged from 8 h to 24 h after USPIO

administration. However, a relatively high dose (10 mg iron/kg) was needed for sufficient USPIO deposition because neovascularization of carotid atherosclerotic lesions occurs at a reduced level compared to aortic atherosclerotic lesions. In addition, studies showed that nanocarriers modified with folic acid can specifically target activated macrophages through specific binding to folic acid receptor β .^{32,33}

Apolipoprotein AI (apoA-I) is the major structural protein in high-density lipoprotein (HDL) particles, which is recognized and taken by macrophages and has anti-inflammatory properties and promotes cholesterol reverse transport (RCT) in macrophages. ApoA-I mimetic peptides can be employed for targeting purpose in the diagnosis/imaging of atherosclerosis.⁸⁴ Cormode et al.²⁸ compared the MRI performance of two apoA-I mimetic peptides (18A—DWLKFYDKVAEKLKEAF, 37pA—DWLKFYDKVAEKLKEAFPDWLFYDKVAEKLKEAF) incorporated on HDL-based contrast agents containing Gd-DTPA-DMPE. MRI imaging showed that both contrast agents enhanced the MRI signal in the atherosclerotic plaques of apoE^{-/-} mice (~90%). Another study, in which the ApoE apolipoprotein peptide P2fA2 (LRKLRKLLR) was incorporated into a reconstituted HDL (rHDL) nanoparticle platform enriched with Gd-based amphiphiles as a plaque-specific MR imaging contrast agent, also showed a stronger MRI signal at the atherosclerotic plaque of apoE^{-/-} mice.²⁹

In the early stages of apoptosis, cells begin to express phosphatidylserine (PS) at the outer leaflet of the phospholipid bilayer, which acts as recognition sites for macrophage digestion. Annexin V (A5) has a high affinity for PS and can therefore be used to target apoptotic foam cells in the atheroma and evaluate plaque vulnerability. The exact affinity of A5 to PS is difficult to measure, partly due to its very tight binding. It was estimated that the protein dissociation constant is in the picomolar to femtomolar range.³⁴ Recombinant A5 has successfully been used to target apoptotic foam cells in atherosclerotic lesions in formats, such as ^{99m}Tc-labelled probes, and SPION- and micelle-conjugates.^{35,36}

5. Targeting plaque-weakening proteases

Atherosclerotic plaque rupture is the primary cause of myocardial infarctions and strokes. Vulnerable plaques are characterized by thin, highly inflamed, and collagen-poor fibrous caps. Proteases are enzymes involved in the digestion of extracellular matrix protein, plaque remodelling and fibrous cap weakening, ultimately leading to plaque destabilization and rupture. By exploiting their enzymatic activity, cleavable ligands can be used to target functionalized nanoparticles to sites of high protease activity. The use of both activity- and substrate-based probes for non-invasive imaging of proteases have been extensively studied. In general, activity-based probes exhibit more rapid and selective uptake in addition to stronger signal contrast compared to substrate-based probes.⁸⁵

Elevated concentration of matrix metalloproteinases (MMPs) is an indicator of plaque weakening as they degrade extracellular matrix proteins, such as fibrin, elastin, collagen, and gelatine. In contrast, some MMPs assist the migration and proliferation of smooth muscle cells; therefore, promoting fibrous cap stability. There are at least 23 MMPs that have been identified, with differential expression of each being correlated with varying pathological states. In advanced atherosclerotic plaques, MMP content is at least 50 nM. However, this value is underestimated due to the unavailability of data for all MMP subtypes.⁸⁶

Potent MMP inhibitors have been used as templates for radiolabelled probes. CGS 25966 and CGS 27023A are N-sulphonyl amino acid

hydroxamates that are non-selective inhibitors of MMP-1 ($K_i = 43$ nM and 33 nM, respectively), MMP-2 ($K_i = 11$ nM and 20 nM, respectively), MMP-3 ($K_i = 34$ nM and 43 nM, respectively), and MMP-9 ($K_i = 27$ nM and 8 nM, respectively), through chelation of the zinc ion in the enzyme active site. PET-compatible ^{18}F -labelled CGS 27023A derivatives were used to assess MMPs *in vitro* and *in vivo*. Fluorogenic inhibition assays showed that the tracer had nanomolar to sub-nanomolar IC_{50} values comparable to the lead structure. Importantly, *in vivo* studies in mice showed that there was no unfavourable unspecific accumulation of the tracer in heart or carotid regions. Biodistribution and plasma protein binding studies will provide further evidence for the clinical viability of ^{18}F -labelled CGS 27023A.³⁷ P947 is an MRI contrast agent composed of a broad-spectrum MMP inhibitor coupled to Gd chelate and DOTA. The P947 molecule is another hydroxamate-type MMP inhibitor. The IC_{50} values of P947 for soluble MMP-1, -2, -3, -8, -9, and -13 were in the micromolar range and were consistent with those of the free peptide; therefore, the contrast moiety did not drastically alter the binding ability of the peptide. The *in vivo* biodistribution assay showed that the compound had a plasma half-life of 30 min and was rapidly cleared, leaving only 2% of the injected dose in the plasma and main organs 1-h post-injection. Regions with large atherosclerotic plaques (e.g. the carotid arteries and aortic arch) contained micromolar concentrations of P947.³⁸

Attention has been brought upon gelatinases (MMP-2 and MMP-9) due to their elevated concentrations under pathological stress and correlation with plaque vulnerability. Deguchi *et al.*³⁹ synthesized an NIRF probe consisting of a gelatinase substrate sequence GGPRQITAG, previously identified from a phage library. The catalytic efficiency K_{cat}/K_m ratio of NIRF probe was measured to be $180\,000\text{ M}^{-1}\text{ s}^{-1}$. The study presented an *in vivo* imaging technique that detects MMP-2 and -9 activities in macrophage-rich plaques. It was highlighted that, however, with the presence of more fibrous plaques, NIRF signal was negligible due to decreased macrophage content.

Another class of enzymes involved in the degradation of intracellular proteins are cysteine proteases. Cathepsins belong to a superfamily of cysteine proteases that utilize acidic lysosomes to degrade intracellular proteins. However, cells such as endothelial cells, SMCs, and macrophages can mobilize them extracellularly as activatable proenzymes. These include cathepsins B, L, S, and K, which are thought to participate in plaque proteolysis.⁴⁷ Among them, cathepsin K (CatK) is one of the most active elastolytic and collagenolytic proteases, localized to the fibrous cap and plaque shoulders. However, antibodies targeted to CatK do not distinguish active CatK from zymogen precursors, which are not proteolytic. To assess this active CatK *in vivo*, a new NIRF probe was developed. Accordingly, the protease-activatable substrate was quenched at baseline but fluoresced upon cleavage by the target enzyme. A highly specific CatK peptide substrate (GHPGGPQGKC), with a modest binding affinity (1.2 μM), was incorporated as the cleavable ligand.⁴⁰ The proline residue at P2 allows for the high specificity for the S2 and S2' site, as well as resistance to proteolysis by CatB, CatF, CatG, CatH, CatL, CatS, CatV, chymotrypsin, and leucocyte elastase. When human carotid atherosclerotic specimens were incubated with the CatK imaging agent, the NIRF signal within the plaque co-localized with CatK and CD68-positive macrophages. Optical imaging identified co-localization of the signal associated with CatK and CD68-positive macrophages, demonstrating the CatK imaging capabilities in human atherosclerosis.⁸⁷ Similar results were seen in a Cy5.5-labelled CatB-specific activatable probe. Kim *et al.*⁸⁸ demonstrated by *ex vivo* imaging that the probe was able to quantitatively assess the effect of anti-atherosclerotic treatments (e.g. statins) through the reduction of CatB activity in macrophage-rich plaques.

6. Targeting biomarkers on thrombus

Thrombosis occurs when the fibrous cap of an unstable atherosclerotic plaque ruptures, releasing clot-promoting components into the circulating blood.⁴ The components involved in the platelet activation and the coagulation cascade (Figure 2) can be targeted for therapeutic and diagnostic applications.

6.1 Activated platelets

P-selectin is an adhesion molecule,⁸⁹ expressed at the surface of activated platelets, which mediates rolling and trapping of leucocytes within the thrombus. P-selectin is also expressed on endothelial cells and plays an essential role in the initial recruitment of leucocytes to the site of injury during inflammation. With its ability to link innate immunity with the inflamed endothelium and coagulation, P-selectin can be used as a molecular target in acute and chronic CVDs.⁹⁰

Sulfated polysaccharides are known as P-selectin ligands. Fucoidan, a sulfated and fucosylated polysaccharide derived from brown algae and seaweed, has been reported to have high affinity for immobilized P-selectin ($K_d = 0.3\text{--}1.2$ nM), along with its lowest non-specific binding when compared with other polysaccharides.⁹¹ Rouzet *et al.*⁹² studied the use of radiolabelled fucoidan ($^{99\text{m}}\text{Tc}$ -fucoidan) as a thrombus imaging agent. The extraction of fucoidan from algae or seaweed results in molecular weight differences and variations in fucose, sulfate, and uronic acid compositions. A solution would be to define structural characteristics that correspond to an optimal action, akin to what was done for heparin.⁹³ Fucoidan was also used to target USPIO nanoparticles to activated platelets, which could then be visualized using MRI. Comparable to $^{99\text{m}}\text{Tc}$ -fucoidan, USPIO-fucoidan was rapidly cleared from circulation, with a mean value of 4.4% of the injected dose 60 min post-injection.⁹⁴

Integrins, such as $\alpha_{\text{IIb}}\beta_3$ (GPIIb/IIIa) and $\alpha_v\beta_3$, are transmembrane receptors that are abundant on activated platelets—more so GPIIb/IIIa, with 50 000 to 80 000 molecules on a platelet, compared to several hundred molecules of $\alpha_v\beta_3$ presented.⁹⁵ The $\alpha_v\beta_3$ -integrin mediates the binding of platelets to vitronectin, a plasma glycoprotein thought to regulate diverse physiological processes. Platelet adhesion and aggregation at sites of vascular injury, caused by vitronectin, contribute to the pathogenesis of atherosclerosis and thrombosis.⁹⁶ Therefore, vitronectin antagonists can be used for diagnosis and treatment by targeting the platelet $\alpha_v\beta_3$. Peptidomimetic vitronectin has been used to direct paramagnetic nanoparticles to $\alpha_v\beta_3$ -integrin for non-invasive assessment of early atherosclerosis.⁴¹ Accordingly, the K_i value for $\alpha_v\beta_3$ -integrin was reported to be in the micromolar range.

Alternatively, the abundance of GPIIb/IIIa receptors on the platelet surface membrane offers more effective platelet targeting strategies. Activated platelets secrete thromboxane A_2 which acts in an autocrine manner, binding to thromboxane receptors on the platelet's own surface and neighbouring platelets. The intra-platelet signalling converts GPIIb/IIIa receptors to their active form to initiate the aggregation. This subset of integrin recognizes a common peptide motif: RGD. As such, several peptides have been engineered to target GPIIb/IIIa using the RGD motif. Linear RGD peptides, such as RGDS, GRGDS, and GRGDSP, have low affinities ($\text{IC}_{50} > 100$ nM) and selectivity.⁹⁷ Cyclization of RGD peptides via disulfide or thioether linkers often results in higher binding affinity and selectivity.⁹⁸ P280 is a cyclic RGD peptide approved by the FDA for the detection of acute deep vein thrombosis. P280 showed specific binding to GPIIb/IIIa and selectively

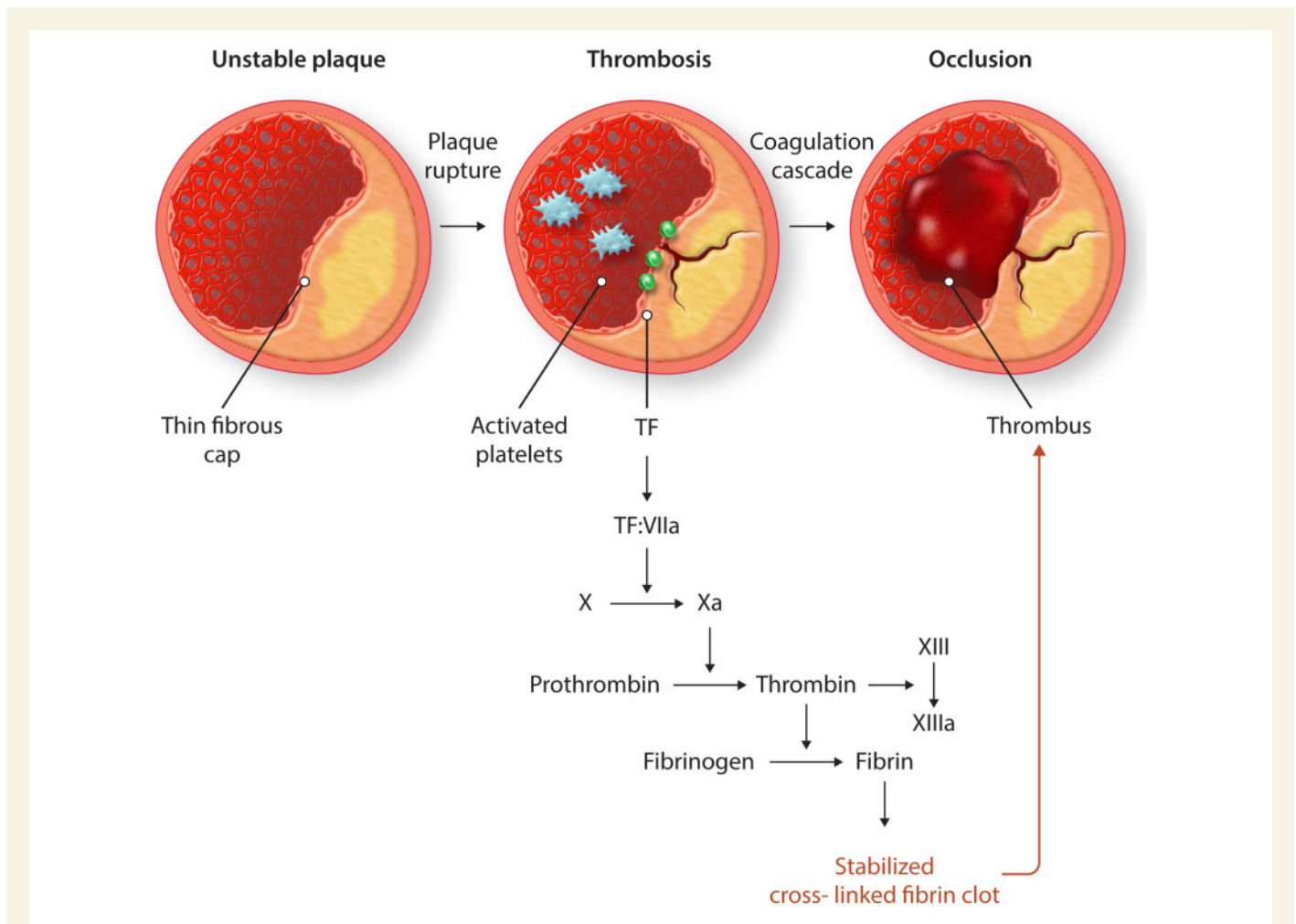


Figure 2 Vulnerable plaque rupture and subsequent thrombus formation causing arterial occlusion. The coagulation cascade (extrinsic pathway) is initiated when plaque contents, primarily tissue factor (TF), are exposed to the circulation, eventually leading to thrombin activation.

accumulated in the fresh thrombi, inhibiting platelet aggregation ($IC_{50} = 79 \text{ nM}$) and fibrinogen binding ($IC_{50} = 6.8 \text{ nM}$).⁹ The sensitivity and specificity of P280 for patients with DVT was 87% and 100%, respectively.⁹⁹ P975, a cyclic RDG peptide (CRGNC) conjugated to Gd-DOTA, was shown to have a K_i value of $1.5 \mu\text{M}$ ($IC_{50} = 2.1 \mu\text{M}$). The addition of the Gd chelate (and linker) caused a slight reduction in affinity of the originator peptide, P977 ($K_i = 1.1 \mu\text{M}$). The specificity for P975 was assessed using eptifibatide—a GPIIb/IIIa antagonist recognized for having high specificity for GPIIb/IIIa and low affinity for other integrins. Following a saturation dose of eptifibatide, administration of P975 caused an initial signal increase of the thrombus for 30 min before rapidly clearing out of circulation.⁴⁴ Incorporation of an aromatic ring into a cyclic peptide can further enhance the binding affinity and selectivity. DuPont Merck Pharmaceuticals originally engineered two antithrombotic agents, DMP728 and DMP757, with nanomolar affinity for GPIIb/IIIa: $IC_{50} = 0.6 \text{ nM}$ and $IC_{50} = 6 \text{ nM}$, respectively.^{45,46} Mousa et al.⁴⁵ combined DMP 728 with a tissue-type plasminogen activator (TPA) or streptokinase (SK). In a dog model, the compound shortened the time to reperfusion and capable of limiting further platelet deposition. Although RGD peptides are able to enhance the accumulation of nanomaterials and therapeutics to thrombosis, they also bind to other integrins (such as $\alpha v\beta 3$,

$\alpha v\beta 5$, and $\alpha v\beta 6$) expressed on cancer cells,¹⁰⁰ thus they are not specific for platelets only.

A single-chain antibody (scFv) which targets specifically to the activated conformation of the GPIIb/IIIa receptor (scFv_{antiGPIIb/IIIa}), binding to the ligand-induced binding site has been used for imaging of thrombosis, inflammation, and cancer.^{101–103} The scFv only consists of heavy and light chain variable region of an IgG, connected by a short peptide; and can be easily modified for conjugation without the loss of its functions.¹⁰⁴ This scFv_{antiGPIIb/IIIa} has been proven to target only activated platelets and does not bind to non-activated platelets *in vitro* and *in vivo*. The scFv_{antiGPIIb/IIIa} has been conjugation onto MBs for ultrasound imaging,⁴⁸ iron oxide nanoparticles for MRI,^{49,105–114} radiotracers for PET imaging and near-infrared dyes for 3D fluorescence imaging of thrombosis.⁴⁸

Monoclonal antibodies or peptides against the GPIIb/IIIa receptors have been used as antithrombotic therapies. Among them, abciximab is one of the most famous chimeric anti-b3 (c7E3 Fab) monoclonal antibodies.¹¹⁵ The representative of the polypeptide is eptifibatide, a cyclic heptapeptide based on the KGD amino acid that is now widely accepted in the market.¹¹⁶ By genetically engineering a fibrinolytic agent, a single-chain urokinase plasminogen activator (scuPA), onto the anti-GPIIb/IIIa scFv, they demonstrate the ability to deliver potent drug payload to the

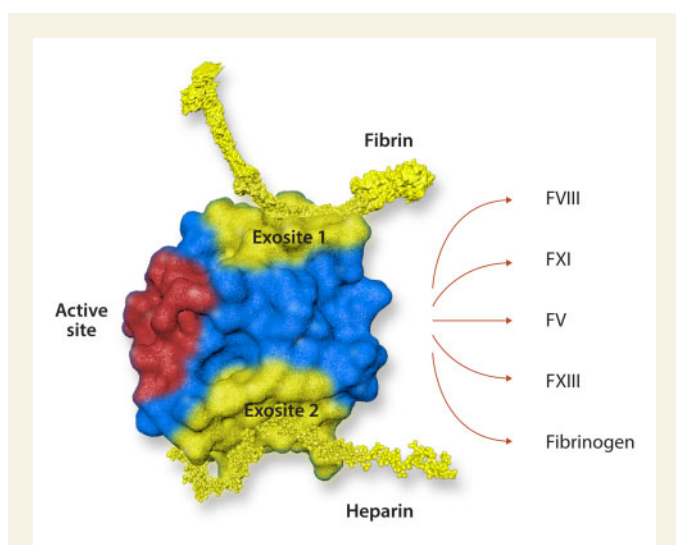


Figure 3 Thrombin—a trypsin-like serine protease—has a multi-functional role in the coagulation cascade as it catalyses the conversion of fibrinogen to fibrin and activates factors V, VIII, XI, and XIII. On the surface of thrombin, exosites I and II are able to interact with ligands, such as fibrin and heparin, that alter the catalytic function of thrombin and allow it to recognize a wide range of factors in the coagulation cascade.

site of thrombosis without bleeding complications.¹¹⁷ Another example is the fusion of an anti-thrombotic agent CD39.^{47,50} The targeted treatment exhibited strong antithrombotic potency *in vivo* using a murine model of acute thrombosis and also without bleeding complications. Due to the slight delayed in exposure and conformational change of activated GPIIb/IIIa on activated platelets, the initial sealing layer of platelets binding to damaged endothelium was not affected; therefore, bleeding was still prevented.⁵⁰

Using an MB conjugated with both scFV_{antiGPIIb/IIIa} and scuPA for a theranostic approach, Wang *et al.*¹¹⁸ demonstrated *in vivo*, using a murine model of acute carotid artery thrombosis, successful diagnosis of thrombus area, followed by real-time monitoring of thrombus breakdown. The same degree of thrombolysis using non-targeted commercially available urokinase led to an increasing bleeding time. However, this theranostic approach only needed a fraction of the drug dose because the targeting scFV_{antiGPIIb/IIIa} homed the MBs to the area of injury, hence did not increase bleeding time.¹¹⁸

The above studies demonstrated the potential to employ biomarkers on activated platelets for targeting purpose in atherosclerosis and thrombosis. However, it should be noted that activated platelets are presented on a thrombus during its early phase, and to a lesser extent on older clots, which could hinder sufficient accumulation of therapeutic and diagnostic agents.⁵¹

6.2 Thrombin

The serine protease, thrombin, has a multifunctional role in biological processes, including thrombogenesis, angiogenesis, and tissue injury. Prothrombin, the inactive form of thrombin, circulates in the plasma at a concentration of 1.4 μM . Exposure of tissue factors to circulating blood begins processes of the extrinsic pathway, which leads to the activation of prothrombin to thrombin. Thrombin activates factors XI, VIII, V, I (fibrinogen), and XIII, as well as protease activated receptors, which cause

platelet activation and aggregation. The average measured concentration of thrombin in actively growing thrombi is 37 nM.¹¹⁹ However, thrombin concentration can be variable, e.g. with highly active patches, it can reach 400–500 nM.^{119,120}

A human thrombin-cleavable peptide ligand (GPXRSGGGK), linked to a near-infrared fluorochrome (Cy5.5) probe, was utilized to image thrombin activity *in vivo*.⁵² The peptide sequence served as a substrate for thrombin and has a reported K_{cat}/K_m of $3.94 \times 10^7 \text{ M}^{-1} \text{ s}^{-1}$ and a circulation time of 20 h.¹²¹ The same thrombin-cleavable peptide ligand was incorporated into silica-capped gold nanoparticles as a novel fluorescence/micro-CT dual imaging probe. Under normal physiological conditions, the near-infrared signal is quenched due to the distance-dependent effect of excited states of the fluorescence Cy5.5. However, in the presence of thrombin, Cy5.5 fluorescence is activated due to rapid cleavage from the thrombin-cleavable ligand. The accumulation of targeted silica-capped gold nanoparticles in an *in situ* thrombotic mouse model was rapid.¹²² Recently, Ta *et al.*^{53,123} developed an activatable magnetic resonance nanosensor as potential imaging agent for detecting and discriminating thrombosis. The nanosensor consisted of an iron oxide core linked with a gadolinium chelate layer via thrombin-cleavable peptides (KKLVPRGSL) and exhibited MRI positive contrast on fresh/acute thrombi while showed negative contrast effect upon binding to old/chronic thrombi.

Along with the active site, thrombin also has other notable structures called exosites I and II (Figure 3).¹²⁴ The substrate specificity of thrombin is regulated by binding of ligands to exosites I and II. Studies have reported independent exosite interactions, in which structurally different exosite-specific ligands produce different effects on the catalytic site.¹²⁵ Dougan *et al.*⁵⁴ investigated two DNA aptamers, oligodeoxynucleotide (ODN) 1 and 2, directed against exosites I and II, respectively. Thrombin binds fibrin via exosite I; therefore, ODN1 is unable to bind to fibrin-bound thrombin, impeding its use as a thrombin-targeting ligand. In contrast, ODN2 binds to exosite II and can form a complex with fibrin-bound thrombin, allowing effective thrombus imaging. *In vitro* results indicated that ODN2 has a relatively high binding affinity for thrombin ($K_d = 0.5 \text{ nM}$). Aptamers are typically non-immunogenic and non-toxic. However, as the characteristic of aptamers, ODN2 was rapidly cleared from circulation and had slow mass transfer in the thrombus in rabbit jugular vein model. Compared to thrombin ligands, such as heparin and glycosaminoglycan, glycoprotein I β (GPI β), a surface membrane protein of platelets, binds strongly and specifically to exosite II. This binding can be inhibited with low molecular weight lignins and benzofurans. Motivated by these phenomena, Mehta *et al.*⁵⁵ synthesized a mimetic agent based on the sulfated tyrosine sequence of GPI β : SbO4L (sulfated β -O4 lignin). SbO4L exhibited potent inhibition ($\text{IC}_{50} = 14 \text{ nM}$), preventing the thrombin-mediated platelet activation and aggregation. SbO4L inhibited factor Xa and factor Xia with an IC_{50} of 10–50 μM , indicating highly selective inhibition.

Page *et al.*¹²⁶ engineered thrombin-responsive constructs—named as restricted interaction peptides (RIPs)—that were capable of non-invasive imaging. The pro-peptide had a sequence composed of labelled-temporin L (TempL) followed by protease-activated receptor-1 (PAR1) activation site, separated by a cleavage site. The PAR1 activation site is a highly sensitive substrate of thrombin and can be used as a thrombin-targeting sequence. TempL is able to bind phospholipid membranes; however, the presence of the thrombin-targeting sequence reduces its affinity for cellular membranes. When proteolysis occurs, the labelled membrane-binding module (TempL) is released and will undergo insertion into cellular membranes.

6.3 Fibrin

Fibrin is an insoluble, trimeric molecule formed during the clotting cascade via thrombin-induced polymerization of fibrinogen, followed by the Factor XIII-mediated crosslinking. The concentration of circulating fibrinogen is 2–4 mg/mL, which shares 98% of its structure with fibrin.¹²⁷ The concentration of circulating fibrin is virtually undetectable but can rapidly increase during pathological conditions, resulting in 100-s-micromolar concentrations. On average, each gram of a clot contains 50 mg of fibrin. Furthermore, fibrin remains a significant component of the thrombus, irrespective of whether the clot is fresh or old.⁵¹

Raut et al.⁵⁹ engineered two human anti-fibrin monoclonal antibodies (mAbs), 1H10 and 5F3, which bind to various domains of the fibrinogen/fibrin moiety. Both mAbs reacted similarly with the E domain of fibrin, however, 1H10 had a higher binding affinity than 5F3 (K_d were 3.9 nM and 4.3 nM, respectively). Another mAb, AP2, was isolated from an antibody phage display library that was designed for the selective recognition of the N-terminal peptide of the fibrin α -chain. AP2 binds to fibrin with an affinity of 44 nM and showed specificity for fibrin over fibrinogen. Binding affinity to N-acetylated fibrin peptides was also undetectable.⁶⁰

TP850, a fibrin α -chain pentapeptide (GPRPP) that binds to the C-terminal of fibrin γ -chain, was shown to have the highest clot-inhibiting activity out of several analogues.¹²⁸ Aruva et al.⁵¹ labelled the pentapeptide with ^{99m}Tc and investigated its use as an imaging agent for DVT and PE using swine models. Data indicated that the affinity of this probe to human fibrin was 8 nM. The high affinity and large number of binding sites (3.8×10^{15} per mg of fibrin) presented allowed sufficient accumulation of radioactivity for reliable detection of thrombi.

A peptide-based MRI contrast agent, EP-2104R, was targeted to fibrin for detection of deposition in atherosclerosis and thrombosis. EP-2104R consisted of an 11-amino acid peptide that binds to fibrin (YQCPYGLCYIQ), linked to 4 Gd-DOTAGA chelates. *In vitro* binding studies determined the K_d of EP-2104R to human fibrin to be 1.6 μ M. Although the binding affinity of EP-2104R was relatively low, the high concentration of fibrin during the clotting process (5–10 mg/mL) enables sufficient binding of EP-2104R to clots. Furthermore, the affinity for the peptide portion of EP-2104R, without the 4 Gd chelates, was 2.5 times greater. Specificity to fibrin over fibrinogen, which circulates at concentrations of 7.5 μ M, is an important characteristic of EP-2104R due to the shared structural homology of fibrin and fibrinogen. EP-2104R has a $K_d = 240 \mu$ M to fibrinogen; therefore, there is a 100-fold higher selectivity for fibrin than for fibrinogen.⁶¹

^{99m}Tc-DI-80B3 (ThromboView[®]) is a diagnostic tool used to detect acute venous thromboembolism by utilizing a very high affinity (1.6 nM) Fab' fragment specific for the D-dimer region of cross-linked fibrin.⁵⁷ ^{99m}Tc-DI-80B3 is able to locate the region of DVT and can differentiate an acute (new formed) clot from an old (inactive) one. However, the main drawback was the lack of distinction between the D-dimer measured from plasma, which has poor specificity for DVT, and D-dimer that is used with ^{99m}Tc-DI-80B3 imaging, creating significant levels of background signal.⁵⁸

6.4 Activated factor XIII

Activated factor XIII (FXIIIa) is an enzyme involved in the late stages of the blood coagulation system. FXIIIa crosslinks polymerized fibrin molecules through forming covalent bonds between glutamine (position 14) and the ϵ -amino group of a lysine residue, thus adding stability to the thrombus. In addition, the integration of plasmin inhibitors into the fibrin structure provides resistance to thrombolytic enzymes. Unlike fibrin,

which is omnipresent during thrombogenesis, the presence of FXIIIa is a characteristic of acute thrombi. Normal plasma concentrations of FXIII are 100-fold less than fibrinogen.¹²⁰

The transglutaminase activity of FXIIIa was utilized to cross-link an α 2-antiplasmin-based peptide-based diagnostic probe with fibrin. The α 2-antiplasmin is a prominent inhibitor of fibrinolysis and is cross-linked with fibrin to increase the resistance of the clot. The A15 peptide sequence N₁₃QEQVSPLTLK₂₄ was used as the primary template for the imaging probe.⁶² FXIIIa incorporates the A15 peptide into the fibrin matrix through covalent bonding. *In vivo* studies highlighted the decline in cross-linking activity as the clot ages.¹²⁹

In addition to FXIII, coagulation factor X (FX) and factor XII (FXII), the plasma proteases that in their active forms (FXa and FXIIa) also plays an important role in the formation of blood clotting, initiating the procoagulant and proinflammatory contact system. Interestingly, the absence/deficiency of FXII can interfere thrombosis but is not associated with bleeding (not impair haemostatic capacity or increase bleeding).¹³⁰ The development of drugs targeting FXII(a), therefore, is a promising and safe approach for thrombosis treatment. Several classes of FXII(a) inhibitors have been developed including recombinant proteins,¹³¹ synthetic peptides,¹³² small molecular weight FXIIa inhibitors,¹³³ antibodies,¹³⁴ and antisense oligonucleotides that knockdown FXII expression.¹³⁵ FX and FXII have not been employed to target nanomaterials to atherosclerosis or thrombosis though.

7. Multi-target

Endoglin (CD105 and TGF- β receptor III) is a receptor-associated glycoprotein involved in multiple TGF- β signalling pathways. Endoglin receptor expression is exclusive to cells found in the vessel walls, such as endothelial cells, macrophages, fibroblasts, and smooth muscle cells. Endoglin presents as a promising molecular target as pathological conditions (e.g. hypoxia or vascular injury) can cause an increase in endoglin expression.¹³⁶ However, studies investigating the targeting of endoglin in atherosclerotic models are yet to be performed. Evidence suggests that bone morphogenetic protein 9 (BMP-9) has a nanomolar binding affinity for endoglin, which is dependent on the glycosylation state of the receptor: $K_d = 2$ nM (low glycosylation) and 10 nM (high glycosylation). Using BMP-9 as a template, peptide ligands could be synthesized and used to functionalize theranostic moieties to endoglin, thus targeting multiple cell types.⁶³

Park et al.⁶⁴ discovered the AP peptide using phage display screening. With the sequence CRKRLDRNC, the peptide selectively binds to atherosclerotic plaques via the IL-4 receptor on endothelial cells, macrophages, and smooth muscle cells. The KRLDRN motif is known to be the core of the binding site of IL-4 to the IL-4 receptor and has a picomolar binding affinity.¹³⁷ The peptide was used to functionalize hydrophobically modified glycol chitosan (HGC), which are effective carrier nanoparticles due to their good biodegradability and biocompatibility, low toxicity, and prolonged drug circulation time.⁶⁴

Stabilin-2 is a multifunctional glycoprotein associated with immunity, expressed predominantly in macrophages and endothelial cells. It can be used as a hyaluronic acid receptor in endocytosis to participate in the clearance of bacteria,¹³⁸ or as a membrane phosphatidylserine (PS) receptor to participate in the phagocytosis of apoptotic cells.¹³⁹ Lee et al.⁶⁵ found that stabilin-2 was widely expressed in atherosclerotic plaques than in normal vessel walls and was present not only in macrophages but also in endothelial and smooth muscle cells in plaques. Using phage

display technology, the group developed a stabilin-2-specific peptide CRTLTVRKC (S2P) and showed that the peptide could efficiently target fluorescence molecule FITC and glycol chitosan nanoparticles to atherosclerotic plaques.

8. Conclusions and perspectives

The high mortality associated with CVDs and the complex pathology of atherosclerosis has led to extensive research aiming to characterize the cellular and molecular events that take place during plaque development and progression. As such, the present review provides an understanding on current strategies for targeting epitopes presented throughout atherosclerosis progresses for the diagnosis and treatment of CVDs. The effectiveness of a targeted ligand carrier system is greatly influenced by two factors: (i) the binding affinity between ligand and target and (ii) the abundance of target throughout distinct stages of atherosclerosis and thrombosis.

Out of the ligands reviewed, antibody-based systems were the most commonly researched due to their high affinity and specificity compared to other targeting ligands. However, their relatively large size can be immunogenic. Constructing antibody fragments can reduce the immunogenicity but compromises binding affinity. A major difficulty associated with the use of antibody and antibody fragments lies in developing reliable chemistry to conjugate them to carrier systems such as nanoparticles and liposomes.

Peptide ligands are another effective alternative that offer certain advantages over antibody- and antibody fragment-based targeting ligands, as their smaller size is better suited to the nanoparticle structure but compromises binding affinity and specificity. In addition, peptide-based ligands have been used widely as targeting ligands due to their synthetic flexibility and low production cost. The sequence and structure can be easily modified to optimize binding, e.g. through cyclization. Due to their size and structure, peptide ligands are less immunogenic than antibodies.

The use of aptamers as targeting ligands is a relatively novel technique but is able to achieve binding affinity and specificity comparable to antibodies at a much smaller molecular size. DNA and RNA aptamers have advantages over antibodies, such as rapid production and non-immunogenicity. Some studies on aptamers directed towards atherosclerosis have been reported. Those which have been studied had typical characteristics of aptamers: rapid clearance by renal filtration and nuclease degradation.¹⁴⁰

As atherosclerosis progresses, there is a shift in the cellular and molecular profile of the plaque. The same phenomenon occurs as thrombus age. This can impact the effectiveness of a targeted nanoparticle as the presence of the molecular or cellular target may vary depending on the stage of the disease. Activated platelets are primarily associated with the early stage of thrombosis, whereas fibrin remains a significant component throughout all stages. Furthermore, differences in cellular activity, such as macrophages, have been correlated with the vulnerability of atherosclerotic plaques. Thus, the choice of target would rely on the intended purpose of the nanoparticle; e.g. the delivery of therapeutic agents to plaques or thrombi, assessing the progression of disease, or assessing vulnerability of rupture.

Although binding affinity of some ligands on their targeted receptor counterparts have been reported, the binding affinity of ligand-conjugated NPs (as a whole) on different components of atherosclerotic plaques requires further research. In addition, there have been no studies

comparing the binding affinities of different ligands to the same target receptor.

Similarly, the binding affinity of the same ligand to target receptors in different nanosystems may also vary, depending on the properties of the nanomaterial such as size, shape, and surface charge. These aspects require more research in the future.

Conflict of interest: none declared.

Funding

This work was supported by the National Health and Medical Research Council (APP1146694 to H.T.T.).

References

- World Health Organization. Cardiovascular Diseases (CVDs) Fact Sheet. 2017. <https://www.afro.who.int/health-topics/cardiovascular-diseases> (6 March 2020, date last accessed).
- Libby P, Ridker PM, Maseri A. Inflammation and atherosclerosis. *Circulation* 2002; **105**:1135–1143.
- Falk E. Pathogenesis of atherosclerosis. *J Am Coll Cardiol* 2006; **47**:C7–C12.
- Virmani R, Kolodgie FD, Burke AP, Farb A, Schwartz SM. Lessons from sudden coronary death: a comprehensive morphological classification scheme for atherosclerotic lesions. *Arterioscler Thromb Vasc Biol* 2000; **20**:1262–1275.
- McCarthy JR. Nanomedicine and cardiovascular disease. *Curr Cardiovasc Imaging Rep* 2010; **3**:42–49.
- Lewis DR, Kamisoglu K, York AW, Moghe PV. Polymer-based therapeutics: nanoassemblies and nanoparticles for management of atherosclerosis. *Wiley Interdiscip Rev Nanomed Nanobiotechnol* 2011; **3**:400–420.
- Kratz JD, Chaddha A, Bhattacharjee S, Goonewardena SN. Atherosclerosis and nanotechnology: diagnostic and therapeutic applications. *Cardiovasc Drugs Ther* 2016; **30**:33–39.
- Pierschbacher MD, Ruoslahti E. Cell attachment activity of fibronectin can be duplicated by small synthetic fragments of the molecule. *Nature* 1984; **309**:30–33.
- Lister-James J, Knight LC, Maurer AH, Bush LR, Moyer BR, Dean RT. Thrombus imaging with a technetium-99m-labeled activated platelet receptor-binding peptide. *J Nucl Med* 1996; **37**:775–781.
- Mann AP, Somasunderam A, Nieves-Alicea R, Li X, Hu A, Sood AK, Ferrari M, Gorenstein DG, Tanaka T. Identification of thioaptamer ligand against E-selectin: potential application for inflamed vasculature targeting. *PLoS One* 2010; **5**:e13050.
- Nahrendorf M, Jaffer FA, Kelly KA, Sosnovik DE, Aikawa E, Libby P, Weissleder R. Noninvasive vascular cell adhesion molecule-1 imaging identifies inflammatory activation of cells in atherosclerosis. *Circulation* 2006; **114**:1504–1511.
- Burtea C, Ballet S, Laurent S, Rousseaux O, Dencausse A, Gonzalez W, Port M, Corot C, Vander Elst L, Muller RN. Development of a magnetic resonance imaging protocol for the characterization of atherosclerotic plaque by using vascular cell adhesion molecule-1 and apoptosis-targeted ultrasmall superparamagnetic iron oxide derivatives. *Arterioscler Thromb Vasc Biol* 2012; **32**:e36–e48.
- Michalska M, Machtoub L, Manthey HD, Bauer E, Herold V, Krohne G, Lykowsky G, Hildenbrand M, Kampf T, Jakob P, Zerneck A, Bauer WR. Visualization of vascular inflammation in the atherosclerotic mouse by ultrasmall superparamagnetic iron oxide vascular cell adhesion molecule-1-specific nanoparticles. *Arterioscler Thromb Vasc Biol* 2012; **32**:2350–2357.
- Bruckman MA, Jiang K, Simpson EJ, Randolph LN, Luyt LG, Yu X, Steinmetz N. Dual-modal magnetic resonance and fluorescence imaging of atherosclerotic plaques *in vivo* using VCAM-1 targeted tobacco mosaic virus. *Nano Lett* 2014; **14**:1551–1558.
- Wang X, Searle AK, Hohmann JD, Liu AL, Abraham M-K, Palasubramaniam J, Lim B, Yao Y, Wallert M, Yu E, Chen Y-C, Peter K. Dual-targeted theranostic delivery of miRs arrests abdominal aortic aneurysm development. *Mol Ther* 2018; **26**:1056–1065.
- Gandhi NS, Coombe DR, Mancera RL. Platelet endothelial cell adhesion molecule 1 (PECAM-1) and its interactions with glycosaminoglycans: 1. Molecular modeling studies. *Biochemistry* 2008; **47**:4851–4862.
- Dziubla TD, Shuvaev VV, Hong NK, Hawkins BJ, Madesh M, Takano H, Simone E, Nakada MT, Fisher A, Albelda SM, Muzykantov VR. Endothelial targeting of semi-permeable polymer nanocarriers for enzyme therapies. *Biomaterials* 2008; **29**:215–227.
- Bertrand M-J, Abran M, Maafi F, Busseuil D, Merlet N, Mihalache-Avrant T, Geoffroy P, Tardif P-L, Abulrob A, Arbabi-Ghahroudi M, Ni F, Sirois M, L'Allier PL, Rhéaume É, Lesage F, Tardif J-C. *In vivo* near-infrared fluorescence imaging of atherosclerosis using local delivery of novel targeted molecular probes. *Sci Rep* 2019; **9**:2670.
- Herbst SM, Klegerman ME, Kim H, Qi J, Shelat H, Wessler M, Moody MR, Yang CM, Ge X, Zou Y, Kopeček JA, Clubb FJ, Kraemer DC, Huang S, Holland CK, McPherson DD, Geng YJ. Delivery of stem cells to porcine arterial wall with

- echogenic liposomes conjugated to antibodies against CD34 and intercellular adhesion molecule-1. *Mol Pharm* 2010;**7**:3–11.
20. Danila D, Partha R, Elrod DB, Lackey M, Casscells SW, Conyers JL. Antibody-labeled liposomes for CT imaging of atherosclerotic plaques: *in vitro* investigation of an anti-ICAM antibody-labeled liposome containing iohexol for molecular imaging of atherosclerotic plaques via computed tomography. *Tex Heart Inst J* 2009;**36**:393–403.
 21. Paulis LE, Jacobs I, van den Akker NM, Geelen T, Molin DG, Starmans LW, Nicolay K, Strijkers G. Targeting of ICAM-1 on vascular endothelium under static and shear stress conditions using a liposomal Gd-based MRI contrast agent. *J Nanobiotechnol* 2012;**10**:25.
 22. Garnacho C, Serrano D, Muro S. A fibrinogen-derived peptide provides intercellular adhesion molecule-1-specific targeting and intraendothelial transport of polymer nanocarriers in human cell cultures and mice. *J Pharmacol Exp Ther* 2012;**340**:638–647.
 23. Yan F, Yang W, Li X, Liu H, Nan X, Xie L, Zhou D, Xie G, Wu J, Qiu B, Liu X, Zheng H. Magnetic resonance imaging of atherosclerosis using CD81-targeted microparticles of iron oxide in mice. *Biomed Res Int* 2015;**2015**:758616.
 24. Amirbekian V, Lipinski MJ, Briley-Saebo KC, Amirbekian S, Aguinaldo JG, Weinreb DB, Vucic E, Frias JC, Hyafil F, Mani V, Fisher EA, Fayad ZA. Detecting and assessing macrophages *in vivo* to evaluate atherosclerosis noninvasively using molecular MRI. *Proc Natl Acad Sci USA* 2007;**104**:961–966.
 25. Wen S, Liu DF, Cui Y, Harris SS, Chen YC, Li KC, Ju SH, Teng GJ. *In vivo* MRI detection of carotid atherosclerotic lesions and kidney inflammation in ApoE-deficient mice by using LOX-1 targeted iron nanoparticles. *Nanomedicine* 2014;**10**:639–649.
 26. Lipinski MJ, Frias JC, Amirbekian V, Briley-Saebo KC, Mani V, Samber D, Abbate A, Aguinaldo JG, Massey D, Fuster V, Vetrovec GW, Fayad ZA. Macrophage-specific lipid-based nanoparticles improve cardiac magnetic resonance detection and characterization of human atherosclerosis. *JACC Cardiovasc Imaging* 2009;**2**:637–647.
 27. Bujold K, Mellal K, Zoccal KF, Rhoads D, Brissette L, Febbraio M, Marleau S, Ong H. EP 80317, a CD36 selective ligand, promotes reverse cholesterol transport in apolipoprotein E-deficient mice. *Atherosclerosis* 2013;**229**:408–414.
 28. Cormode DP, Chandrasekar R, Delshad A, Briley-Saebo KC, Calcagno C, Barazza A, Mulder WJ, Fisher EA, Fayad ZA. Comparison of synthetic high density lipoprotein (HDL) contrast agents for MR imaging of atherosclerosis. *Bioconjug Chem* 2009;**20**:937–943.
 29. Chen W, Vucic E, Leupold E, Mulder WJ, Cormode DP, Briley-Saebo KC, Barazza A, Fisher EA, Dathe M, Fayad ZA. Incorporation of an apoE-derived lipopeptide in high-density lipoprotein MRI contrast agents for enhanced imaging of macrophages in atherosclerosis. *Contrast Media Mol Imaging* 2008;**3**:233–242.
 30. Chung EJ, Milnar LB, Nord K, Sugimoto MJ, Wonder E, Alenghat FJ, Fang Y, Tirrell M. Monocyte-targeting supramolecular micellar assemblies: a molecular diagnostic tool for atherosclerosis. *Adv Healthc Mater* 2015;**4**:367–376.
 31. Luehmans HP, Pressly ED, Detering L, Wang C, Pierce R, Woodard PK, Gropler RJ, Hawker CJ, Liu Y. PET/CT imaging of chemokine receptor CCR5 in vascular injury model using targeted nanoparticle. *J Nucl Med* 2014;**55**:629–634.
 32. Rollett A, Reiter T, Nogueira P, Cardinale M, Loureiro A, Gomes A, Cavaco-Paulo A, Moreira A, Carmo AM, Guebitz G. Folic acid-functionalized human serum albumin nanocapsules for targeted drug delivery to chronically activated macrophages. *Int J Pharm* 2012;**427**:460–466.
 33. Piscaer TM, Müller C, Mindt TL, Lubberts E, Verhaar JA, Krenning EP, Schibli R, De Jong M, Weinans H. Imaging of activated macrophages in experimental osteoarthritis using folate-targeted animal single-photon-emission computed tomography/computed tomography. *Arthritis Rheum* 2011;**63**:1898–1907.
 34. Tait JF, Gibson DF, Smith C. Measurement of the affinity and cooperativity of annexin V-membrane binding under conditions of low membrane occupancy. *Anal Biochem* 2004;**329**:112–119.
 35. Smith BR, Heverhagen J, Knopp M, Schmalbrock P, Shapiro J, Shiomi M, Moldovan NI, Ferrari M, Lee SC. Localization to atherosclerotic plaque and biodistribution of biochemically derivatized superparamagnetic iron oxide nanoparticles (SPIONs) contrast particles for magnetic resonance imaging (MRI). *Biomed Microdevices* 2007;**9**:719–727.
 36. van Tilborg GA, Vucic E, Strijkers GJ, Cormode DP, Mani V, Skajaa T, Reutelingsperger CP, Fayad ZA, Mulder WJ, Nicolay K. Annexin A5-functionalized bimodal nanoparticles for MRI and fluorescence imaging of atherosclerotic plaques. *Bioconjug Chem* 2010;**21**:1794–1803.
 37. Wagner S, Breyholz HJ, Holtke C, Faust A, Schober O, Schafers M, Kopka K. A new 18F-labelled derivative of the MMP inhibitor CGS 27023A for PET: radiosynthesis and initial small-animal PET studies. *Appl Radiat Isot* 2009;**67**:606–610.
 38. Ouimet T, Lancelot E, Hyafil F, Rienzo M, Deux F, Lemaître M, Duquesnoy S, Garot J, Roques BP, Michel JB, Corot C, Ballet S. Molecular and cellular targets of the MRI contrast agent P947 for atherosclerosis imaging. *Mol Pharm* 2012;**9**:850–861.
 39. Deguchi JO, Aikawa M, Tung CH, Aikawa E, Kim DE, Ntziachristos V, Weissleder R, Libby P. Inflammation in atherosclerosis: visualizing matrix metalloproteinase action in macrophages *in vivo*. *Circulation* 2006;**114**:55–62.
 40. Lecaille F, Weidauer E, Juliano MA, Bromme D, Lalmanach G. Probing cathepsin K activity with a selective substrate spanning its active site. *Biochem J* 2003;**375**:307–312.
 41. Winter PM, Neubauer AM, Caruthers SD, Harris TD, Robertson JD, Williams TA, Schmieder AH, Hu G, Allen JS, Lacy EK, Zhang H, Wickline SA, Lanza GM. Endothelial alpha(v)beta3 integrin-targeted fumagillin nanoparticles inhibit angiogenesis in atherosclerosis. *Arterioscler Thromb Vasc Biol* 2006;**26**:2103–2109.
 42. Ruoslahti E. RGD and other recognition sequences for integrins. *Annu Rev Cell Dev Biol* 1996;**12**:697–715.
 43. Lister-Jones J, Vallabhajosula S, Moyer BR, Pearson DA, McBride BJ, De Rosch MA, Bush LR, Machac J, Dean RT. Pre-clinical evaluation of technetium-99m platelet receptor-binding peptide. *J Nucl Med* 1997;**38**:105–111.
 44. Klink A, Lancelot E, Ballet S, Vucic E, Fabre JE, Gonzalez W, Medina C, Corot C, Mulder WJ, Mallat Z, Fayad ZA. Magnetic resonance molecular imaging of thrombosis in an arachidonic acid mouse model using an activated platelet targeted probe. *Arterioscler Thromb Vasc Biol* 2010;**30**:403–410.
 45. Mousa SA, Bozarth JM, Forsythe MS, Lorelli W, Thoolen MJ, Ramachandran N, Jackson S, De Grado W, Reilly TM. Antiplatelet efficacy and specificity of DMP728, a novel platelet GPIIb/IIIa receptor antagonist. *Cardiology* 1993;**83**:374–382.
 46. Harris TD, Rajopadhye M, Damphousse PR, Glowacka D, Yu K, Bourque JP, Barrett JA, Damphousse DJ, Heminway SJ, Lazewatsky J, Mazaika T, Carroll TR. Tc-99m-labeled fibrinogen receptor antagonists: design and synthesis of cyclic RGD peptides for the detection of thrombi. *Bioorg Med Chem Lett* 1996;**6**:1741–1746.
 47. Garcia-Touchard A, Henry TD, Sangiorgi G, Spagnoli LG, Mauriello A, Conover C, Schwartz RS. Extracellular proteases in atherosclerosis and restenosis. *Arterioscler Thromb Vasc Biol* 2005;**25**:1119–1127.
 48. Wang X, Peter K. Molecular imaging of atherothrombotic diseases: seeing is believing. *Arterioscler Thromb Vasc Biol* 2017;**37**:1029–1040.
 49. Ta HT, Li Z, Hagemeyer C, Cowin G, Palasubramaniam J, Peter K, Whittaker AK. Self-confirming molecular imaging of activated platelets via iron oxide nanoparticles displaying unique dual MRI contrast. *Atherosclerosis* 2017;**263**:e146.
 50. Hohmann JD, Wang X, Krajewski S, Selan C, Haller CA, Straub A, Chaikof EL, Nandurkar HH, Hagemeyer CE, Peter K. Delayed targeting of CD39 to activated platelet GPIIb/IIIa via a single-chain antibody: breaking the link between antithrombotic potency and bleeding? *Blood* 2013;**121**:3067–3075.
 51. Aruva MR, Daviau J, Sharma SS, Thakur ML. Imaging thromboembolism with fibrin-avid 99mTc-peptide: evaluation in swine. *J Nucl Med* 2006;**47**:155–162.
 52. Jaffer FA, Tung CH, Gerszten RE, Weissleder R. *In vivo* imaging of thrombin activity in experimental thrombi with thrombin-sensitive near-infrared molecular probe. *Arterioscler Thromb Vasc Biol* 2002;**22**:1929–1935.
 53. Ta HT, Arndt N, Wu Y, Lim HJ, Landeen S, Zhang R, Kamato D, Little PJ, Whittaker AK, Xu ZP. Activatable magnetic resonance nanosensor as a potential imaging agent for detecting and discriminating thrombosis. *Nanoscale* 2018;**10**:15103–15115.
 54. Dougan H, Weitz JI, Stafford AR, Gillespie KD, Klement P, Hobbs JB, Lyster DM. Evaluation of DNA aptamers directed to thrombin as potential thrombus imaging agents. *Nucl Med Biol* 2003;**30**:61–72.
 55. Mehta AY, Thakkar JN, Mohammed BM, Martin EJ, Brophy DF, Kishimoto T, Desai UR. Targeting the GPIIb/IIIa binding site of thrombin to simultaneously induce dual anticoagulant and antiplatelet effects. *J Med Chem* 2014;**57**:3030–3039.
 56. Stefanelli VL, Barker TH. The evolution of fibrin-specific targeting strategies. *J Mater Chem B* 2015;**3**:1177–1186.
 57. Macfarlane D, Socrates A, Eisenberg P, Larcos G, Roach P, Gerometta M, Smart R, Tsui W, Scott AM. Imaging of deep venous thrombosis in patients using a radiolabelled anti-D-dimer Fab' fragment (99mTc-DI-DD3B6/22-80B3): results of a phase I trial. *Eur J Nucl Med Mol Imaging* 2009;**36**:250–259.
 58. Douketis JD, Ginsberg JS, Haley S, Julian J, Dwyer M, Levine M, Eisenberg PR, Smart R, Tsui W, White RH, Morris TA, Kaatz S, Comp PC, Crowther MA, Kearon C, Kassis J, Bates SM, Schulman S, Desjardins L, Taillefer R, Begelman SM, Gerometta M. Accuracy and safety of (99m)Tc-labeled anti-D-dimer (DI-80B3) Fab' fragments (ThromboView(R)) in the diagnosis of deep vein thrombosis: a phase II study. *Thromb Res* 2012;**130**:381–389.
 59. Raut S, Gaffney PJ. Evaluation of the fibrin binding profile of two anti-fibrin monoclonal antibodies. *Thromb Haemost* 1996;**76**:56–64.
 60. Putelli A, Kiefer JD, Zadory M, Matasi M, Neri D. A fibrin-specific monoclonal antibody from a designed phage display library inhibits clot formation and localizes to tumors *in vivo*. *J Mol Biol* 2014;**426**:3606–3618.
 61. Overoye-Chan K, Koerner S, Looby RJ, Kolodziej AF, Zech SG, Deng Q, Chasse JM, McMurry TJ, Caravan P. EP-2104R: a fibrin-specific gadolinium-Based MRI contrast agent for detection of thrombus. *J Am Chem Soc* 2008;**130**:6025–6039.
 62. Jaffer FA, Tung CH, Wykrzykowska JJ, Ho NH, Houg AK, Reed GL, Weissleder R. Molecular imaging of factor XIIIa activity in thrombosis using a novel, near-infrared fluorescent contrast agent that covalently links to thrombi. *Circulation* 2004;**110**:170–176.
 63. Alt A, Miguel-Romero L, Donderis J, Aristorena M, Blanco FJ, Round A, Rubio V, Bernabeu C, Marina A. Structural and functional insights into endoglin ligand recognition and binding. *PLoS One* 2012;**7**:e29948.
 64. Park K, Hong HY, Moon HJ, Lee BH, Kim IS, Kwon IC, Rhee K. A new atherosclerotic lesion probe based on hydrophobically modified chitosan nanoparticles functionalized by the atherosclerotic plaque targeted peptides. *J Control Release* 2008;**128**:217–223.

65. Lee GY, Kim JH, Oh GT, Lee BH, Kwon IC, Kim IS. Molecular targeting of atherosclerotic plaques by a stabilin-2-specific peptide ligand. *J Control Release* 2011;**155**: 211–217.
66. Doyle B, Caplice N. Plaque neovascularization and antiangiogenic therapy for atherosclerosis. *J Am Coll Cardiol* 2007;**49**:2073–2080.
67. Fujiwara M, Matoba T, Koga J-I, Okahara A, Funamoto D, Nakano K, Tsutsui H, Egashira K. Nanoparticle incorporating Toll-like receptor 4 inhibitor attenuates myocardial ischaemia–reperfusion injury by inhibiting monocyte-mediated inflammation in mice. *Cardiovasc Res* 2019;**115**:1244–1255.
68. Tokutome M, Matoba T, Nakano Y, Okahara A, Fujiwara M, Koga J-I, Nakano K, Tsutsui H, Egashira K. Peroxisome proliferator-activated receptor-gamma targeting nanomedicine promotes cardiac healing after acute myocardial infarction by skewing monocyte/macrophage polarization in preclinical animal models. *Cardiovasc Res* 2018;**115**:419–431.
69. Atukorale PU, Covarrubias G, Bauer L, Karathanasis E. Vascular targeting of nanoparticles for molecular imaging of diseased endothelium. *Adv Drug Deliv Rev* 2017;**113**:141–156.
70. Nishiyama A, Shikata C, Kimura N, Imanishi A, Hirai N, Ohta M, Takeda N. Risk factors for coronary artery sclerosis in patients with diabetes. *Exp Clin Cardiol* 2005;**10**: 108–110.
71. Kelly KA, Allport JR, Tsourkas A, Shinde-Patil VR, Josephson L, Weissleder R. Detection of vascular adhesion molecule-1 expression using a novel multimodal nanoparticle. *Circ Res* 2005;**96**:327–336.
72. Sun X, Li W, Zhang X, Qi M, Zhang Z, Zhang XE, Cui Z. *In vivo* targeting and imaging of atherosclerosis using multifunctional virus-like particles of simian virus 40. *Nano Lett* 2016;**16**:6164–6171.
73. Jubeli E, Moine L, Vergnaud-Gauduchon J, Barratt G. E-selectin as a target for drug delivery and molecular imaging. *J Control Release* 2012;**158**:194–206.
74. Davies MJ, Gordon JL, Gearing AJ, Pigott R, Woolf N, Katz D, Kyriakopoulos A. The expression of the adhesion molecules ICAM-1, VCAM-1, PECAM, and E-selectin in human atherosclerosis. *J Pathol* 1993;**171**:223–229.
75. Hidalgo A, Peired AJ, Wild M, Vestweber D, Frenette PS. Complete identification of E-selectin ligands on neutrophils reveals distinct functions of PSGL-1, ESL-1, and CD44. *Immunity* 2007;**26**:477–489.
76. Rohlena J, Volger OL, van Buul JD, Hekking LH, van Gils JM, Bonta PI, Fontijn RD, Post JA, Hordijk PL, Horrevoets AJ. Endothelial CD81 is a marker of early human atherosclerotic plaques and facilitates monocyte adhesion. *Cardiovasc Res* 2009;**81**: 187–196.
77. Thapa N, Hong HY, Sangeetha P, Kim IS, Yoo J, Rhee K, Oh GT, Kwon IC, Lee BH. Identification of a peptide ligand recognizing dysfunctional endothelial cells for targeting atherosclerosis. *J Control Release* 2008;**131**:27–33.
78. Seneviratne AN, Sivagurunathan B, Monaco C. Toll-like receptors and macrophage activation in atherosclerosis. *Clin Chim Acta* 2012;**413**:3–14.
79. MacNeill BD, Jang I-K, Bouma BE, Iftimia N, Takano M, Yabushita H, Shishkov M, Kauffman CR, Houser SL, Aretz HT, DeJoseph D, Halpern EF, Tearney GJ. Focal and multi-focal plaque distributions in patients with macrophage acute and stable presentations of coronary artery disease. *J Am Coll Cardiol* 2004;**44**:972–979.
80. Kashiwagi M, Imanishi T, Tsujioka H, Ikejima H, Kuroi A, Ozaki Y, Ishibashi K, Komukai K, Tanimoto T, Ino Y, Kitabata H, Hirata K, Akasaka T. Association of monocyte subsets with vulnerability characteristics of coronary plaques as assessed by 64-slice multidetector computed tomography in patients with stable angina pectoris. *Atherosclerosis* 2010;**212**:171–176.
81. Szmítko PE, Wang C-H, Weisel RD, de Almeida JR, Anderson TJ, Verma S. New markers of inflammation and endothelial cell activation: part I. *Circulation* 2003;**108**: 1917–1923.
82. Weissleder R, Nahrendorf M, Pittet MJ. Imaging macrophages with nanoparticles. *Nature Mater* 2014;**13**:125–138.
83. Marleau S, Harb D, Bujold K, Avallone R, Iken K, Wang Y, Demers A, Sirois MG, Febbraio M, Silverstein RL, Tremblay A, Ong H. EP 80317, a ligand of the CD36 scavenger receptor, protects apolipoprotein E-deficient mice from developing atherosclerotic lesions. *FASEB J* 2005;**19**:1869–1871.
84. Navab M, Reddy ST, Van Lenten BJ, Buga GM, Hough G, Wagner AC, Fogelman AM. High-density lipoprotein and 4F peptide reduce systemic inflammation by modulating intestinal oxidized lipid metabolism: novel hypotheses and review of literature. *Arterioscler Thromb Vasc Biol* 2012;**32**:2553–2560.
85. Blum G, Weimer RM, Edgington LE, Adams W, Bogoy M. Comparative assessment of substrates and activity based probes as tools for non-invasive optical imaging of cysteine protease activity. *PLoS One* 2009;**4**:e6374.
86. Hartung D, Schafers M, Fujimoto S, Levkau B, Narula N, Kopka K, Virmani R, Reutelingsperger C, Hofstra L, Kolodgie FD, Petrov A, Narula J. Targeting of matrix metalloproteinase activation for noninvasive detection of vulnerable atherosclerotic lesions. *Eur J Nucl Med Mol Imaging* 2007;**34**: S1–S8.
87. Jaffer FA, Kim DE, Quinti L, Tung CH, Aikawa E, Pande AN, Kohler RH, Shi GP, Libby P, Weissleder R. Optical visualization of cathepsin K activity in atherosclerosis with a novel, protease-activatable fluorescence sensor. *Circulation* 2007;**115**: 2292–2298.
88. Kim DE, Kim JY, Schellingerhout D, Shon SM, Jeong SW, Kim EJ, Kim WK. Molecular imaging of cathepsin B proteolytic enzyme activity reflects the inflammatory component of atherosclerotic pathology and can quantitatively demonstrate the antiatherosclerotic therapeutic effects of atorvastatin and glucosamine. *Mol Imaging* 2009;**8**:291–301.
89. Kappelmaier J, Nagy B. The interaction of selectins and PSGL-1 as a key component in thrombus formation and cancer progression. *Biomed Res Int* 2017;**2017**:6138145.
90. Merten M, Thiagarajan P. P-selectin in arterial thrombosis. *Z Kardiol* 2004;**93**: 855–863.
91. Bachelet L, Bertholon I, Lavigne D, Vassy R, Jandrot-Perrus M, Chaubet F, Letourneur D. Affinity of low molecular weight fucoidan for P-selectin triggers its binding to activated human platelets. *Biochim Biophys Acta* 2009;**1790**:141–146.
92. Rouzet F, Bachelet-Violette L, Alsac JM, Suzuki M, Meulemans A, Louedec L, Petiet A, Jandrot-Perrus M, Chaubet F, Michel JB, Le Guludec D, Letourneur D. Radiolabeled fucoidan as a p-selectin targeting agent for *in vivo* imaging of platelet-rich thrombus and endothelial activation. *J Nucl Med* 2011;**52**:1433–1440.
93. Shriver Z, Capila I, Venkataraman G, Sasisekharan R. Heparin and heparan sulfate: analyzing structure and microheterogeneity. *Handb Exp Pharmacol* 2012;**159**:159–176.
94. Suzuki M, Bachelet-Violette L, Rouzet F, Beilvert A, Autret G, Maire M, Menager C, Louedec L, Choqueux C, Saboural P, Haddad O, Chauvierre C, Chaubet F, Michel JB, Serfaty JM, Letourneur D. Ultrasmall superparamagnetic iron oxide nanoparticles coated with fucoidan for molecular MRI of intraluminal thrombus. *Nanomedicine (Lond)* 2015;**10**:73–87.
95. Bennett JS. Structure and function of the platelet integrin α IIb β 3. *J Clin Invest* 2005;**115**:3363–3369.
96. Bennett JS, Berger BW, Billings PC. The structure and function of platelet integrins. *J Thromb Haemost* 2009;**7**: 200–205.
97. Basani RB, D'Andrea G, Mitra N, Vilaire G, Richberg M, Kowalska MA, Bennett JS, Poncz M. RGD-containing peptides inhibit fibrinogen binding to platelet α IIb β 3 by inducing an allosteric change in the amino-terminal portion of α IIb. *J Biol Chem* 2001;**276**:13975–13981.
98. Zhou Y, Chakraborty S, Liu S. Radiolabeled cyclic RGD peptides as radiotracers for imaging tumors and thrombosis by SPECT. *Theranostics* 2011;**1**:58–82.
99. Bates SM, Lister-Jones J, Julian JA, Taillefer R, Moyer BR, Ginsberg JS. Imaging characteristics of a novel technetium Tc 99m-labeled platelet glycoprotein IIb/IIIa receptor antagonist in patients with acute deep vein thrombosis or a history of deep vein thrombosis. *Arch Intern Med* 2003;**163**:452–456.
100. Liu S. Radiolabeled cyclic RGD peptide bioconjugates as radiotracers targeting multiple integrins. *Bioconjug Chem* 2015;**26**:1413–1438.
101. Ta HT, Prabhu S, Leitner E, Jia F, von Elverfeldt D, Jackson KE, Heidt T, Nair AKN, Pearce H, von Zur Muhlen C, Wang X, Peter K, Hagemeyer CE. Enzymatic single-chain antibody tagging: a universal approach to targeted molecular imaging and cell homing in cardiovascular disease. *Circ Res* 2011;**109**:365–373.
102. von Zur Muhlen C, Sibson NR, Peter K, Campbell SJ, Wilainam P, Grau GE, Bode C, Choudhury RP, Anthony DC. A contrast agent recognizing activated platelets reveals murine cerebral malaria pathology undetectable by conventional MRI. *J Clin Invest* 2008;**118**:1198–1207.
103. Yap ML, McFadyen JD, Wang X, Zia NA, Hohmann JD, Ziegler M, Yao Y, Pham A, Harris M, Donnelly PS, Hogarth PM, Pietersz GA, Lim B, Peter K. Targeting activated platelets: a unique and potentially universal approach for cancer imaging. *Theranostics* 2017;**7**:2565–2574.
104. Pietersz GA, Wang X, Yap ML, Lim B, Peter K. Therapeutic targeting in nanomedicine: the future lies in recombinant antibodies. *Nanomedicine* 2017;**12**:1873–1889.
105. Taussky D, Barkati M, Campeau S, Zerouali K, Nadiri A, Saad F, Delouya G. Changes in periprostatic adipose tissue induced by 5 α -reductase inhibitors. *Andrology* 2017;**5**:511–515.
106. Gaston E, Fraser JF, Xu ZP, Ta HT. Nano- and micro-materials in the treatment of internal bleeding and uncontrolled hemorrhage. *Nanomedicine* 2018;**14**:507–519.
107. Ta H, Prabhu S, Leitner E, Jia F, Putnam K, Bassler N, Peter K, Hagemeyer C. Targeted molecular imaging and cell homing in cardiovascular disease via antibody-sorting. *Atherosclerosis* 2015;**241**:e26.
108. Ta H, Prabhu S, Leitner E, Putnam K, Jia F, Bassler N, Peter K, Hagemeyer C. A novel biotechnological approach for targeted regenerative cell therapy and molecular imaging of atherothrombosis. *Heart Lung Circ* 2010;**19**:S10.
109. Ta HT, Li Z, Hagemeyer C, Wu Y, Lim HJ, Wang W, Wei J, Cowin G, Whittaker AK, Peter K. Novel bionanotechnological solutions based on metal oxide and metal to preserve and assess organs for transplantation. *Cryobiology* 2018;**81**:233.
110. Ta HT, Li Z, Wu Y, Cowin G, Zhang S, Yago A, Whittaker AK, Xu ZP. Effects of magnetic field strength and particle aggregation on relaxivity of ultra-small dual contrast iron oxide nanoparticles. *Mater Res Express* 2017;**4**:116105.
111. Ta HT, Peter K, Hagemeyer CE. Enzymatic antibody tagging: toward a universal biocompatible targeting tool. *Trends Cardiovasc Med* 2012;**22**:105–111.
112. Ta HT, Prabhu S, Leitner E, Jia F, Putnam K, Bassler N, Peter K, Hagemeyer C. Antibody-sorting: a universal approach towards targeted molecular imaging and cell homing in cardiovascular disease. *Circ Res* 2010;**107**:e37–e38.
113. Wu Y, Yang Y, Zhao W, Xu ZP, Little PJ, Whittaker AK, Zhang R, Ta HT. Novel iron oxide-cerium oxide core-shell nanoparticles as a potential theranostic material for ROS related inflammatory diseases. *J Mater Chem B* 2018;**6**:4937–4951.
114. Zhang Y, Koradia A, Kamato D, Popat A, Little PJ, Ta HT. Treatment of atherosclerotic plaque: perspectives on theranostics. *J Pharm Pharmacol* 2019;**71**:1029–1043.
115. Mousa SA. Antiplatelet therapies: from aspirin to GPIIb/IIIa-receptor antagonists and beyond. *Drug Discov Today* 1999;**4**:552–561.

116. Collier BS. Anti-GPIIb/IIIa drugs: current strategies and future directions. *Thromb Haemost* 2001;**86**:427–443.
117. Wang X, Palasubramaniam J, Gkanatsas Y, Hohmann JD, Westein E, Kanojia R, Alt K, Huang D, Jia F, Ahrens I, Medcalf RL, Peter K, Hagemeyer CE. Towards effective and safe thrombolysis and thromboprophylaxis: preclinical testing of a novel antibody-targeted recombinant plasminogen activator directed against activated platelets. *Circ Res* 2014;**114**:1083–1093.
118. Wang X, Gkanatsas Y, Palasubramaniam J, Hohmann JD, Chen YC, Lim B, Hagemeyer CE, Peter K. Thrombus-targeted theranostic microbubbles: a new technology towards concurrent rapid ultrasound diagnosis and bleeding-free fibrinolytic treatment of thrombosis. *Theranostics* 2016;**6**:726–738.
119. Mutch NJ, Robbie LA, Booth NA. Human thrombi contain an abundance of active thrombin. *Thromb Haemost* 2001;**86**:1028–1034.
120. Kattula S, Byrnes JR, Martin SM, Holle LA, Cooley BC, Flick MJ, Wolberg AS. Factor XIII in plasma, but not in platelets, mediates red blood cell retention in clots and venous thrombus size in mice. *Blood Adv* 2018;**2**:25–35.
121. Rijkers DT, Wielders SJ, Tesser GI, Hemker HC. Design and synthesis of thrombin substrates with modified kinetic parameters. *Thromb Res* 1995;**79**:491–499.
122. Kwon SP, Jeon S, Lee SH, Yoon HY, Ryu JH, Choi D, Kim JY, Kim J, Park JH, Kim DE, Kwon IC, Kim K, Ahn CH. Thrombin-activatable fluorescent peptide incorporated gold nanoparticles for dual optical/computed tomography thrombus imaging. *Biomaterials* 2018;**150**:125–136.
123. Yusuf NNM, McCann A, Little PJ, Ta HT. Non-invasive imaging techniques for the differentiation of acute and chronic thrombosis. *Thromb Res* 2019;**177**:161–171.
124. Crawley JT, Zanardelli S, Chion CK, Lane DA. The central role of thrombin in hemostasis. *J Thromb Haemost* 2007;**5**(Suppl 1):95–101.
125. Verhamme IM, Olson ST, Tollefsen DM, Bock PE. Binding of exosite ligands to human thrombin. Re-evaluation of allosteric linkage between thrombin exosites I and II. *J Biol Chem* 2002;**277**:6788–6798.
126. Page MJ, Lourenco AL, David T, LeBeau AM, Cattaruzza F, Castro HC, VanBrocklin HF, Coughlin SR, Craik CS. Non-invasive imaging and cellular tracking of pulmonary emboli by near-infrared fluorescence and positron-emission tomography. *Nat Commun* 2015;**6**:8448.
127. Francis CW, Connaghan DG, Scott WL, Marder VJ. Increased plasma concentration of cross-linked fibrin polymers in acute myocardial infarction. *Circulation* 1987;**75**:1170–1177.
128. Kawasaki K, Miyano M, Hirase K, Iwamoto M. Amino acids and peptides. XVIII. Synthetic peptides related to N-terminal portion of fibrin alpha-chain and their inhibitory effect on fibrinogen/thrombin clotting. *Chem Pharm Bull (Tokyo)* 1993;**41**:975–977.
129. Tung CH, Ho NH, Zeng Q, Tang Y, Jaffer FA, Reed GL, Weissleder R. Novel factor XIII probes for blood coagulation imaging. *Chembiochem* 2003;**4**:897–899.
130. Mackman N. Role of tissue factor in hemostasis, thrombosis, and vascular development. *Arterioscler Thromb Vasc Biol* 2004;**24**:1015–1022.
131. May F, Krupka J, Fries M, Thielmann I, Pragst I, Weimer T, Panousis C, Nieswandt B, Stoll G, Dickneite G, Schulte S, Nolte MW. FXIIa inhibitor rHA-Infestin-4: safe thromboprotection in experimental venous, arterial and foreign surface-induced thrombosis. *Br J Haematol* 2016;**173**:769–778.
132. Baeriswyl V, Calzavarini S, Chen S, Zorzi A, Bologna L, Angelillo-Scherrer A, Heinis C. A synthetic factor XIIa inhibitor blocks selectively intrinsic coagulation initiation. *ACS Chem Biol* 2015;**10**:1861–1870.
133. Bouckaert C, Serra S, Rondelet G, Dolusić E, Wouters J, Dogné JM, Frédéric R, Pochet L. Synthesis, evaluation and structure-activity relationship of new 3-carboxamide coumarins as FXIIa inhibitors. *Eur J Med Chem* 2016;**110**:181–194.
134. Matafonov A, Leung PY, Gailani AE, Grach SL, Puy C, Cheng Q, Sun MF, McCarty OJ, Tucker EI, Kataoka H, Renne T, Morrissey JH, Gruber A, Gailani D. Factor XII inhibition reduces thrombus formation in a primate thrombosis model. *Blood* 2014;**123**:1739–1746.
135. Yau JW, Liao P, Fredenburgh JC, Stafford AR, Revenko AS, Monia BP, Weitz JL. Selective depletion of factor XI or factor XII with antisense oligonucleotides attenuates catheter thrombosis in rabbits. *Blood* 2014;**123**:2102–2107.
136. Lopez-Novoa JM, Bernabeu C. The physiological role of endoglin in the cardiovascular system. *Am J Physiol Heart Circ Physiol* 2010;**299**:H959–H974.
137. Zhang JL, Simeonowa I, Wang Y, Sebald W. The high-affinity interaction of human IL-4 and the receptor alpha chain is constituted by two independent binding clusters. *J Mol Biol* 2002;**315**:399–407.
138. Jung MY, Park SY, Kim IS. Stabilin-2 is involved in lymphocyte adhesion to the hepatic sinusoidal endothelium via the interaction with α M β 2 integrin. *J Leukoc Biol* 2007;**82**:1156–1165.
139. Park S-Y, Jung M-Y, Kim I-S. Stabilin-2 mediates homophilic cell–cell interactions via its FAS1 domains. *FEBS Lett* 2009;**583**:1375–1380.
140. Keefe AD, Pai S, Ellington A. Aptamers as therapeutics. *Nat Rev Drug Discov* 2010;**9**:537–550.